ORNL/SPR-2023/2847

Milestone Report on Microstructure of Irradiated Sensors and Coupling Adhesive Bonds

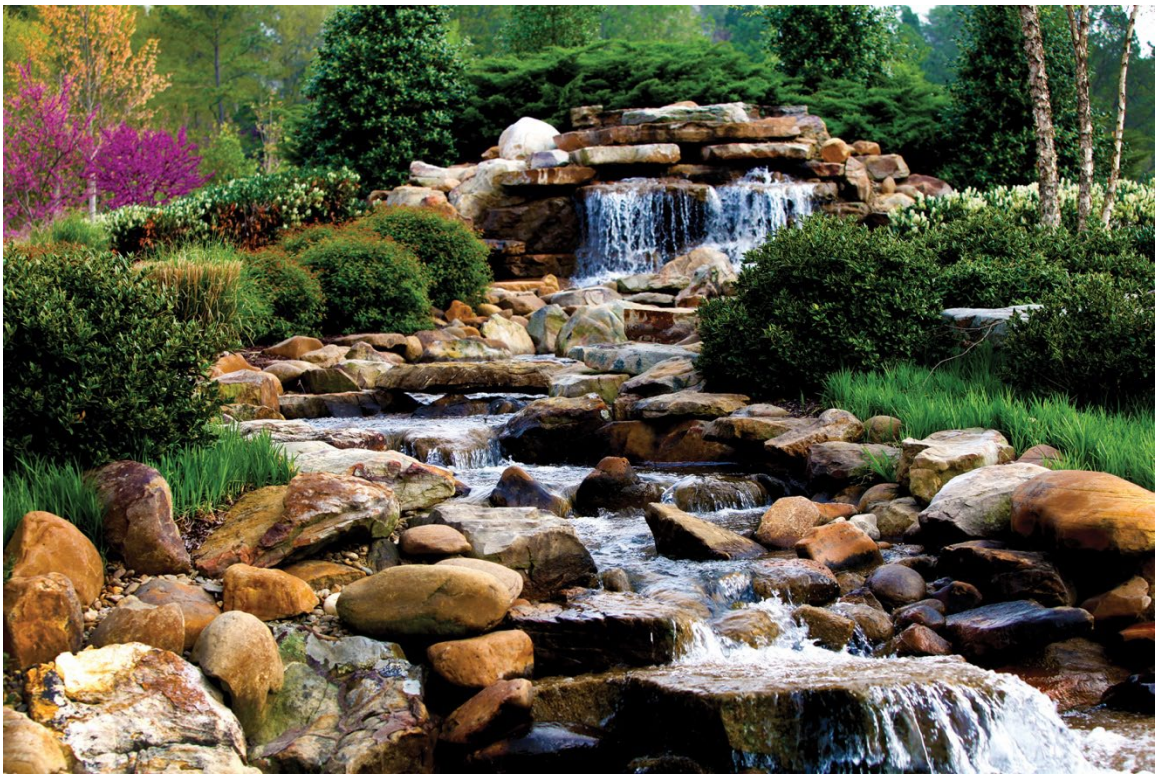

Chad M. Parish

J. Travis Dixon

James Wall

February 2023

OAK RIDGE National Laboratory

ORNL IS MANAGED BY UT-BATTELLE LLC FOR THE US DEPARTMENT OF ENERGY

ORNL/SPR-2023/2847

Materials Science and Technology Division

MILESTONE REPORT ON MICROSTRUCTURE OF IRRADIATED SENSORS AND COUPLING ADHESIVE BONDS

NSUF Milestone Report M3UA-22OR0803012

Chad M. Parish (ORNL)

J. Travis Dixon (ORNL)

James Wall (EPRI)

February 2023

Prepared by

OAK RIDGE NATIONAL LABORATORY

Oak Ridge, TN 37831

managed by

UT-BATTELLE LLC

for the

US DEPARTMENT OF ENERGY

under contract DE-AC05-00OR22725

CONTENTS

Table of Contents

ABSTRACT

This report describes the ORNL aspects of an NSUF project in collaboration between EPRI, ORNL, and NCSU. Preliminary characterizations at ORNL LAMDA laboratory on piezoelectric sensors and bonds before and after NCSU PULSTAR reactor irradiation. Five pre-irradiation and seven post-irradiation samples have been examined by scanning electron microscopy and related methods so far. Samples consisted of (Pb,Bi)(Sc,Ti)O_3 or $LiNbO_3$ ceramics. Bonding layers consisted of epoxy, zirconia, alumina, aluminosilicate, or a complex soda-lime type slurry.

1. INTRODUCTION

This report is to fulfill NSUF Milestone Report M3UA-22OR0803012. This is a Nuclear Science User Facilities (NSUF) project from the Electric Power Research Institute (EPRI). Piezoelectric sensors, mounted with different bonding layers to aluminum substrates, and then neutron irradiated at the PULSTAR facility (https://nrp.ne.ncsu.edu/) at North Carolina State University (NCSU). The goal is to characterize the substrate/piezo bonds before and after irradiation.

Samples examined thus far at ORNL are listed in Table 1. Five unirradiated (control) samples and seven irradiated samples have been examined. Samples were determined by energy dispersive X-ray spectroscopy (EDS) to consist of either Pb-Bi-Sc-Ti-O or Nb-O. These are interpreted to be $(PbTiO_3)_x$-$(BiScO_3)_{(1-x)}$, lead titanate-bismuth scanadate "PBSTO," and $LiNbO_3$, lithium niobate. Crystal structures are rendered in Figure 1.

Table 1. List of examined sample and examination methods, to date.

Status	ID	Piezoelectric	Bonding (elements)	Bonding (interpretation)	Electrode	SEM	SEM-EDS	SEM-EBSD
Unirradiated	1	(Pb,Bi)(Sc,Ti)-O	Si-Al-K-Na-O	Soda slurry	Ag	Y	Y	Y
	5	(Pb,Bi)(Sc,Ti)-O	Al-Si-O	Aluminosilicate	Ag	Y	Y	Y
	11	(Pb,Bi)(Sc,Ti)-O	Al-O	Alumina	Ag	Y	Y	Y
	12	(Pb,Bi)(Sc,Ti)-O	Zr-(Si-Ca-Al-Na-)O	Zirconia	Ag	Y	Y	Y
	13	(Pb,Bi)(Sc,Ti)-O	C-O-S	Epoxy	Ag	Y	Y	
Irradiated	1	(Pb,Bi)(Sc,Ti)-O	Si-Al-K-Na-O	Soda slurry	Ag	Y	Y	
	3	(Li-)Nb-O	Missing	—	Au-Cr	Y	Y	
	4	(Pb,Bi)(Sc,Ti)-O	Al-(Si-Na-K)-O	Alumina	Ag	Y	Y	
	5	(Pb,Bi)(Sc,Ti)-O	Zr-(Si-Ca-Al-Na-)O	Zirconia	Ag	Y	Y	Y
	6	(Pb,Bi)(Sc,Ti)-O	C-O-S	Epoxy	Ag	Y	Y	
	7	(Li-)Nb-O	C-O-S	Epoxy	Au-Cr	Y	Y	
	8	(Li-)Nb-O	C-O-S	Epoxy	Au-Cr	Y	Y	

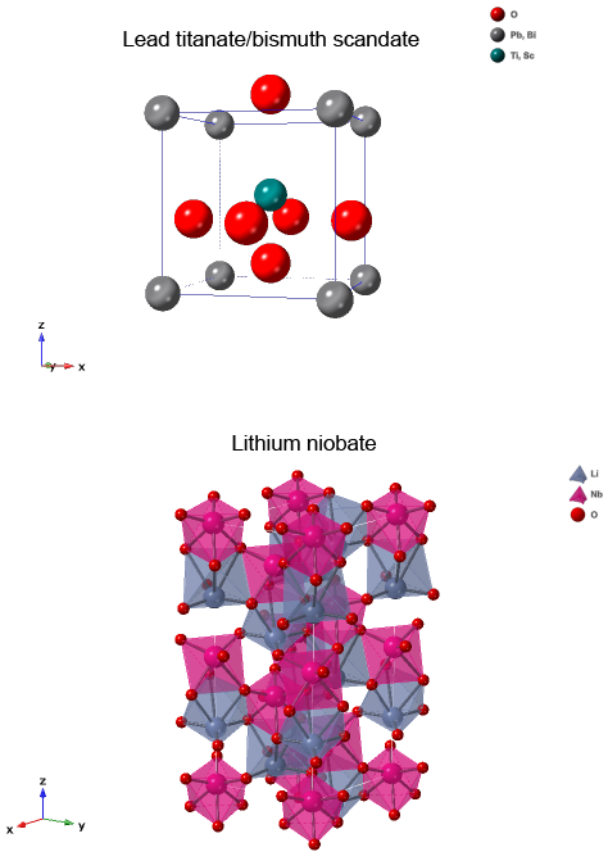

Figure 1. CrystalMaker™ renderings of the piezoelectrics' crystal structures.

2. SAMPLE PREPARATION AND EXPERIMENTAL DETAILS

Samples, irradiated or unirradiated, arrived at ORNL in the form of thin piezoelectric disks ~13 mm in diameter bonded to aluminum substrates ~25 mm in diameter by 10 mm tall. Unirradiated samples were prepared in the ORNL central metallography laboratory and irradiated samples in the LAMDA contamination zone metallography laboratory. The samples were embedded as-received in conductive room-temperature-setting epoxy to ensure the piezoelectric disks would not fall off the aluminum substrate during subsequent handling. Once the epoxy set, the samples were sectioned in half with a low-speed diamond saw, and then one half of each specimen was re-mounted to examine the cut face, again in conductive cold-setting epoxy, and then polished metallographically to colloidal silica for an EBSD-quality polish. After polishing, samples were coated with evaporated carbon using a Cressington carbon coater, and then examined in a Tescan MIRA3 GMH SEM equipped with Oxford SDD EDS and Oxford Symmetry EBSD. Figure 2 illustrates the cutting geometry for cross-sectional samples.

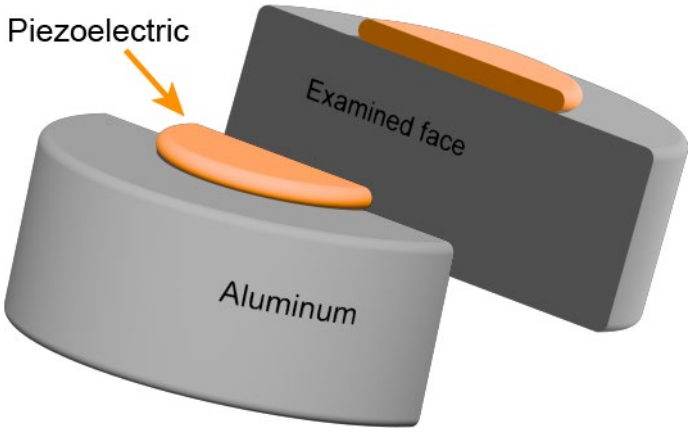

Figure 2. Sample geometry and cutting orientation for cross-sections.

3. SURVEY OF SEM RESULTS

3.1 UNIRRADIATED

Unirradiated Samples #1, 5, 11, 12, and 13 were examined via SEM and SEM-EDS. Figure 3 illustrates the geometry of the cross-sections. Specifically, the epoxy mount is ~32 mm in diameter, the aluminum substrate ~10 mm thick, the piezoelectric disk around 0.5 mm, and the bonding layer <0.5 mm. As seen in Figure 4, the bond is ~150 µm thick, the piezoceramic disk ~400 µm thick, and the bond bulges out around the edge of the disk. The disk is also seen to be porous (black spots, Figure 4-Figure 5). Within the center of the piezoelectric, distinct grains are visible, along with significant porosity. Within individual grains, there appear to be fine piezoelectric domains and high densities of domain walls, Figure 5. The bonding region is imaged in Figure 6, but relatively few details are visible. Note the bright particles in the aluminum (Figure 6, left) are strengthening precipitates expected from aluminum alloy.

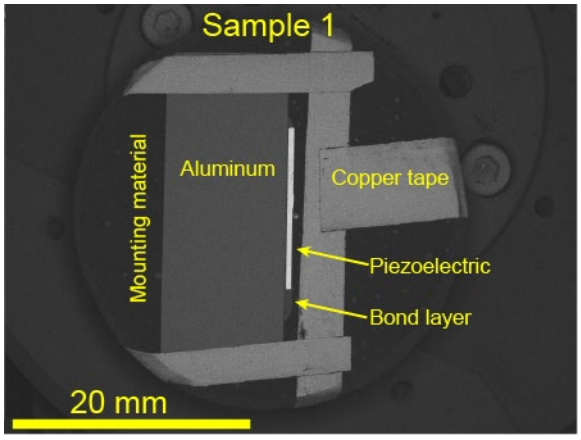

Figure 3. Backscatter electron image of Unirradiated Sample #1 cross-sectioned in its epoxy mount, on the aluminum substrate and mounted with copper tape. Solder ball is not visible in this cut.

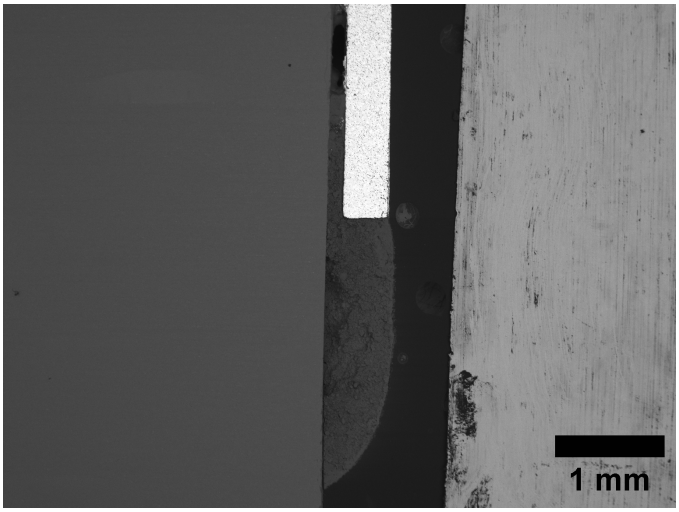

Figure 4. Backscatter electron image of Unirradiated Sample #1, showing details of the bond and piezoceramic.

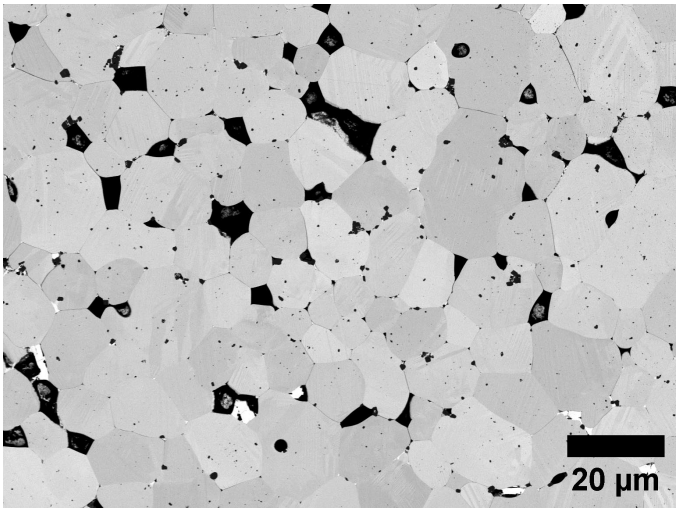

Figure 5. Backscatter electron image of Unirradiated Sample #1, showing details in the middle of the piezoelectric region.

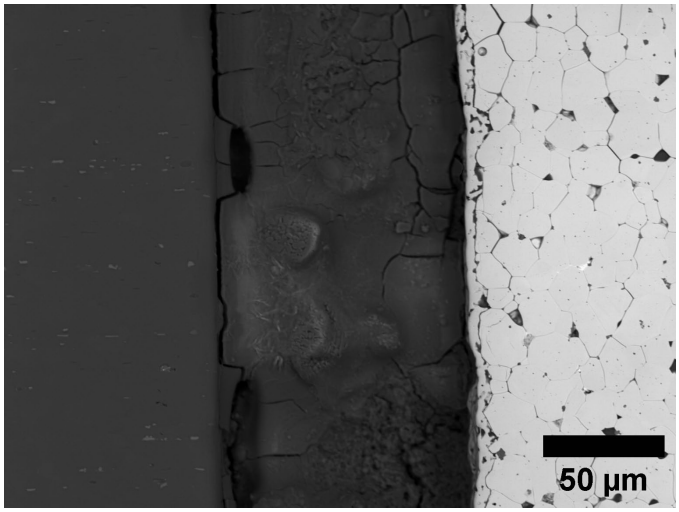

Figure 6. Backscatter electron image of Unirradiated Sample #1, showing details in the bond.

X-ray mapping of Unirradiated Sample 1 finds that the piezoelectric had chemistry of Pb-Bi-Ti-Sc-O and the bonding layer has chemistry Al-Si-Na-K-O. Although standardless EDS quantifications are not precise, it's possible to estimate, from the integrated area spectrum, that the piezoelectric layer is close to an approximate composition of $(PbTiO_3)_{2/3}(BiScO_3)_{1/3}$ or $(PbTiO_3)_{3/5}(BiScO_3)_{2/5}$, very roughly. In the PTO-BSO system, the composition $\sim(PbTiO_3)_{0.66}(BiScO_3)_{0.34}$ is a morphotropic phase boundary (MPB), so this x=0.34 composition of $(PbTiO_3)_{(1-x)}(BiScO_3)_x$ is probably the manufactured target composition, because MPBs tend to show superior piezoelectric properties.

The bonding layer shows mostly Si, with Al as second-most and K and Na being trace. X-ray maps, computed by integrating the peaks and subtracting the backgrounds and overlaps (Oxford Instruments "TruMap™" algorithm) are given in Figure 7. The substrate is Al, the metallographic mounting epoxy C, the piezoelectric disk Pb-Bi-Sc-Ti-O, the bonding layer Al-Si-K-Na-O, and the electrodes on top and bottom of the disk Ag. A high magnification map of the bonding layer, Figure 8, shows that the Al-O and Si-K-Na-O appear as separate regions. Figure 7 and Figure 8 show small packets of Sc-rich material within the piezoelectric.

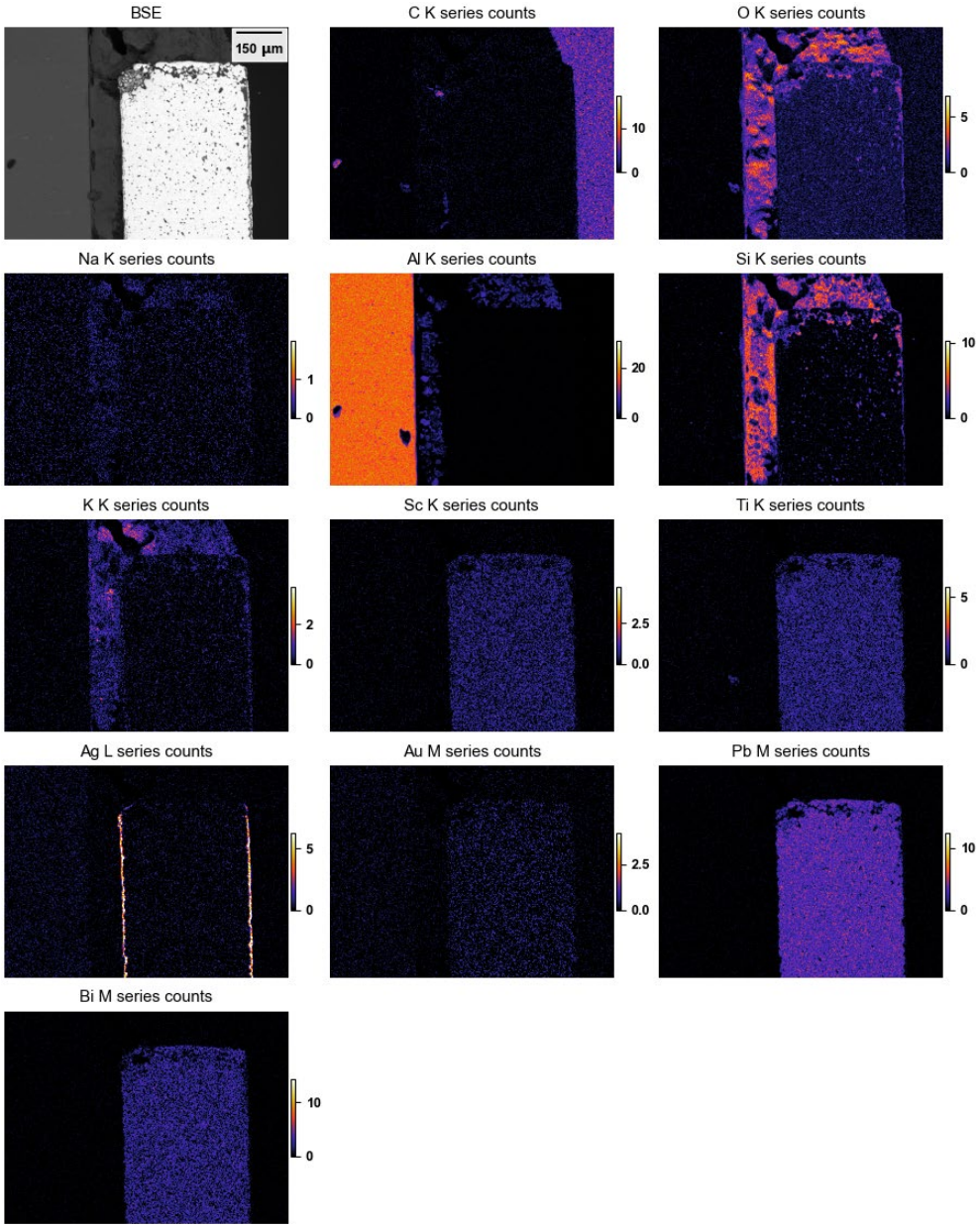

Figure 7. EDS integrated elemental lines extracted from a 15 kV spectrum image from Unirradiated Sample 1.

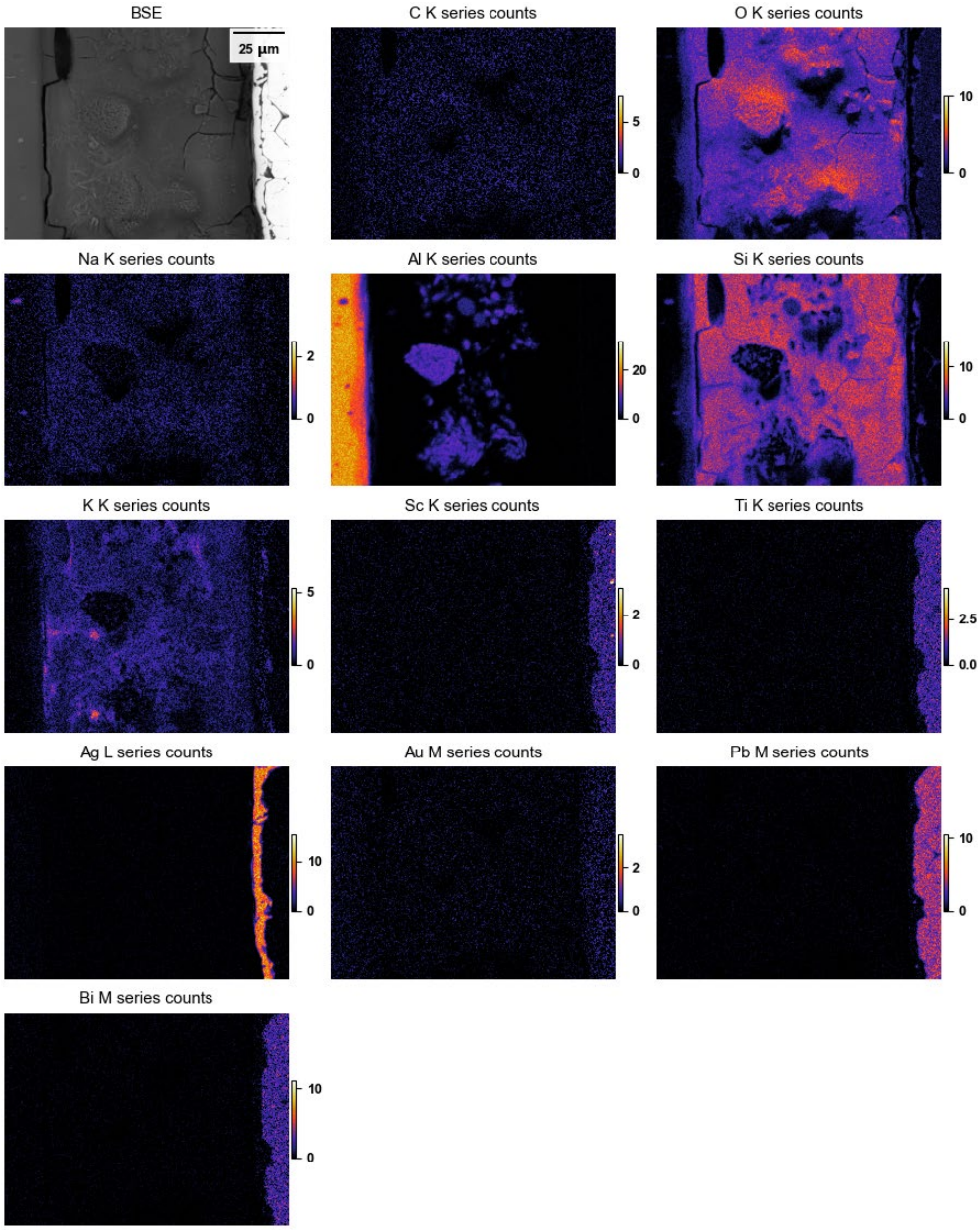

Figure 8. EDS integrated elemental lines extracted from a 15 kV spectrum image from Unirradiated Sample 1 (higher magnification).

Electron backscatter diffraction from the aluminum substrate, across the bonding layer, and into the piezoelectric disk, indexed the aluminum as aluminum metal (unsurprisingly); silver also indexed to Al, because the identical crystal structures cannot be differentiated via EBSD, so only Al was used as a crystal card, not Ag, and both are labelled "FCC (Al/Ag)." The piezoelectric indexed reasonably well as ICSD crystal card #186424, $(PbTiO_3)_{0.64}(BiScO_3)_{0.36}$, space group P 4/mmm #99. It's vital to point out that the perovskite PTO-based system shows many similar crystal structures, so the exact crystal structure cannot be determined with confidence via electron scattering, and X-ray scattering would be more reliable. However, within the boundaries of expecting pseudosymmetry artifacts, this P 4/mmm card worked well. The EBSD results are summarized in Figure 9. Broadly, the aluminum substrate is well-indexed and the grains highly bambooed, probably from extrusion processing. The bonding layer shows a few small particles indexed as Al_2O_3 but is mostly unindexed, indicating

some combination of amorphous material, material too soft to polish to EBSD quality, and/or material whose crystal structure is immediately damaged by the electron beam. Small grains of Ag are present in the electrode, and then the piezoelectric disk shows clear, mostly equiaxed grains with complex domain structures and pseudosymmetry mis-indexing.

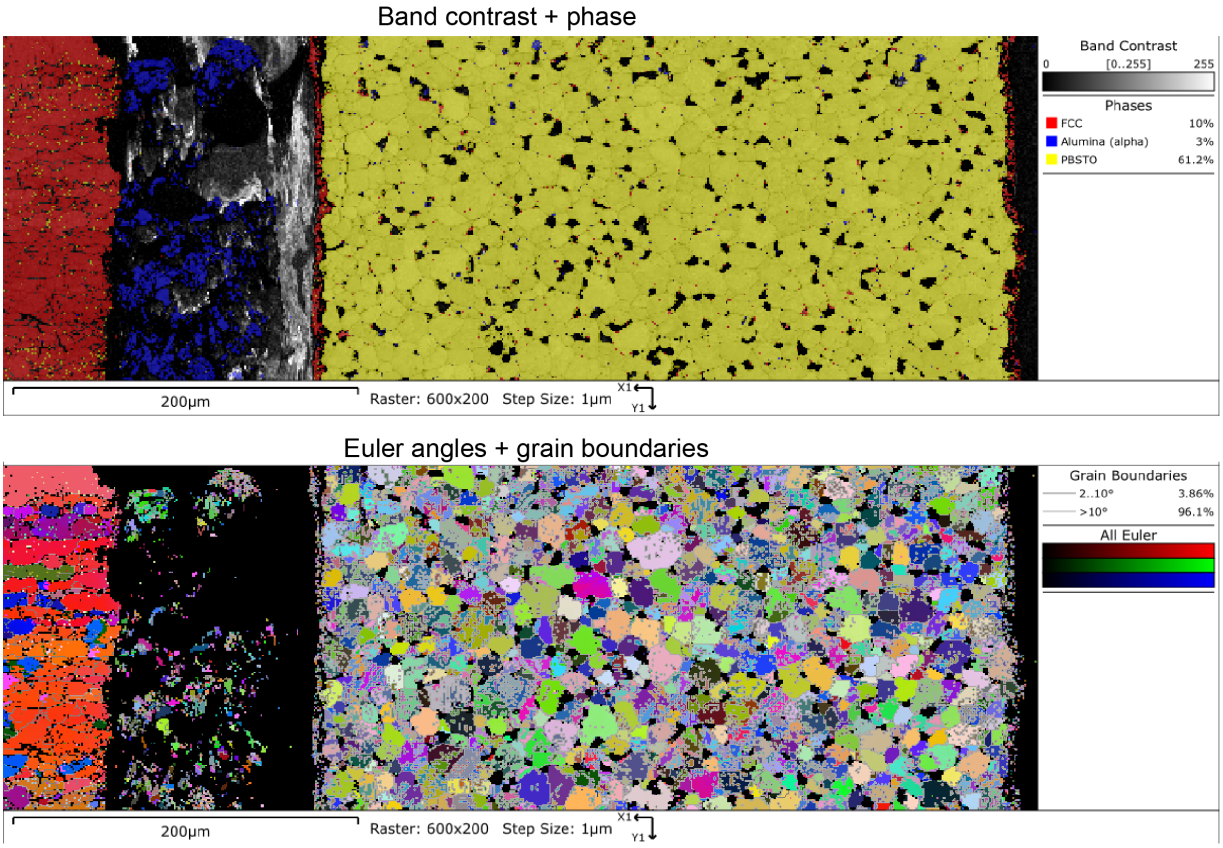

Figure 9. EBSD results from Unirradiated Sample 1. Red phase: FCC, Al or Ag. Blue phase, Al_2O_3. Yellow phase: PBSTO (Pb-Bi-Sc-Ti-O).

After examination of Irradiated Sample #4, below in Section 3.2 revealed unexpected Na-O features (see below), this Unirradiated Sample #1 was re-examined after several months of storage in room air. Needle-like features had grown across the surface of the piezoelectric, Figure 10-Figure 11. EDS mapping found these needles to be Na-K-O rich, Figure 12. This is probably due to reactions between humidity and the reactive metals Na-K; see Irradiated Sample #4, in Section 3.2 below, for comparison and contrast.

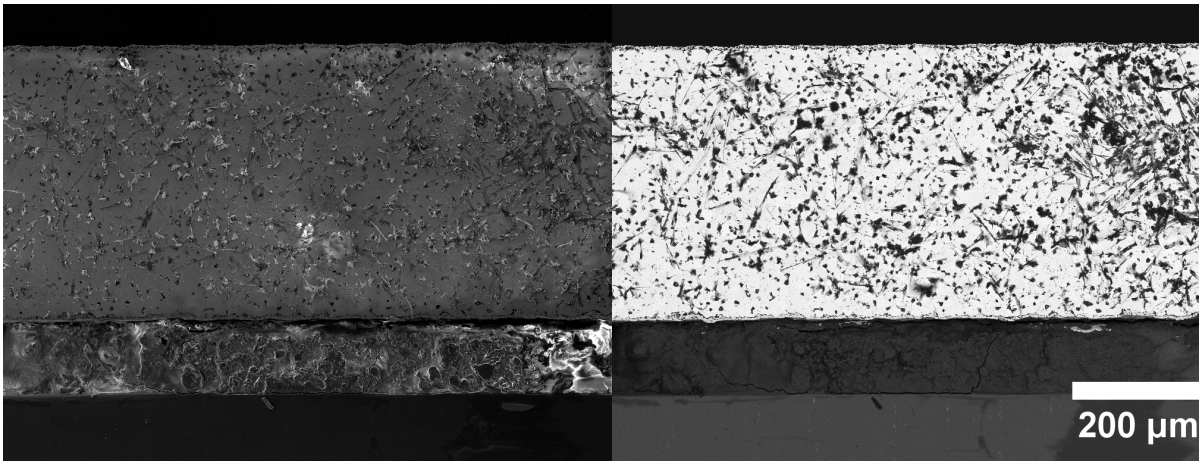

Figure 10. Secondary electron (left) and backscatter electron (right) image of Unirradiated Sample #1 after several months of storage in room air, showing the Na-K-O "needles" growing across the piezoceramic.

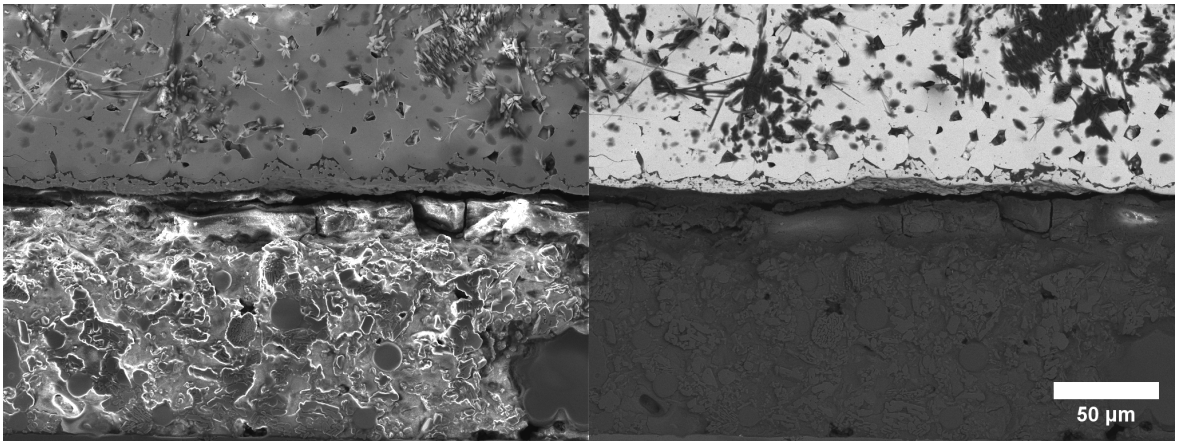

Figure 11. Secondary electron (left) and backscatter electron (right) image of Unirradiated Sample #1 after several months of storage in room air, showing the Na-K-O "needles" growing across the piezoceramic.

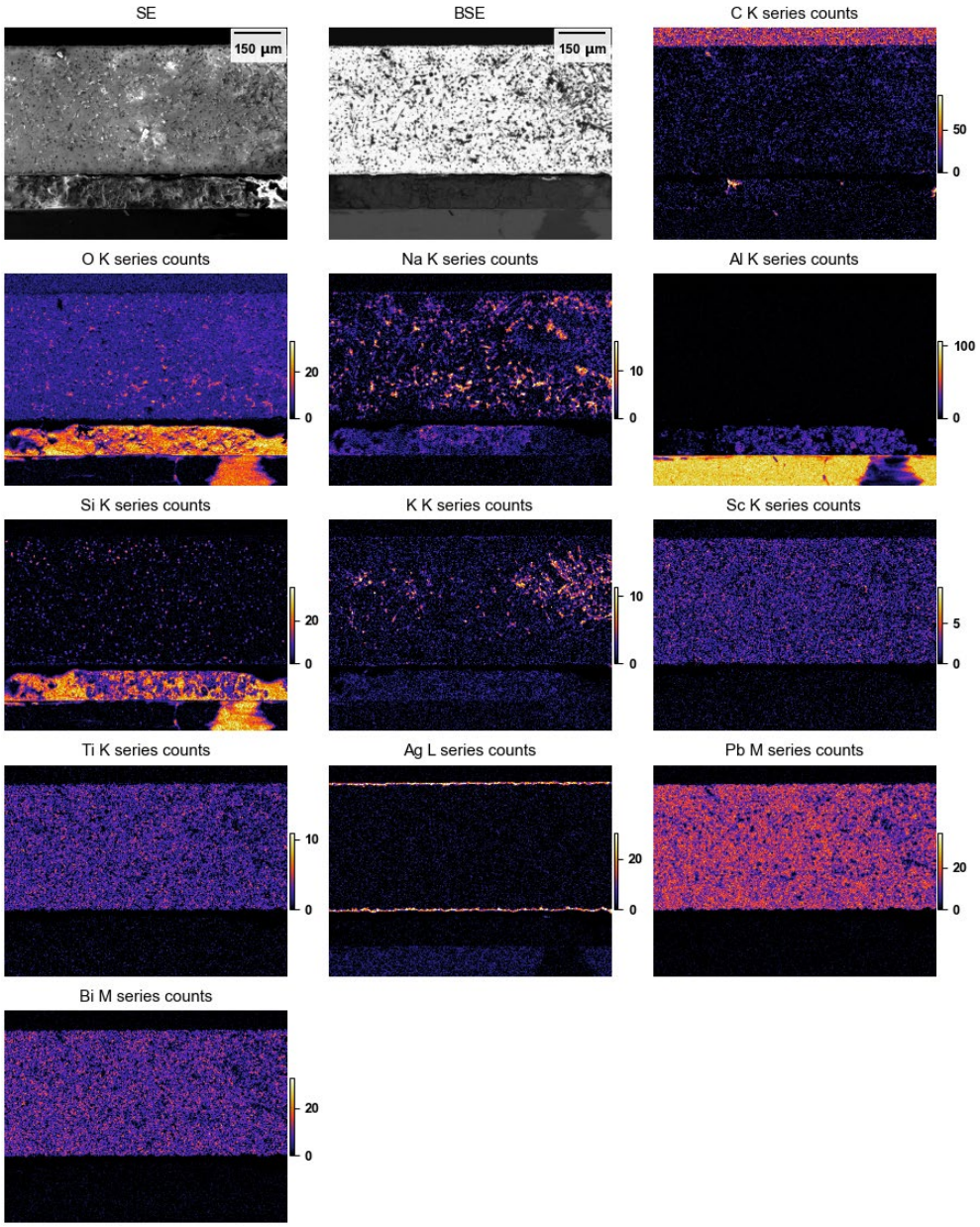

Figure 12. EDS integrated elemental lines extracted from a 10 kV spectrum image from Unradiated Sample #1, showing the Na–K-O rich needles.

Results from Unirradiated Sample 5 are essentially the same, although the bond layer is Al-Si without (or with negligible) Na-K. The gross structure — disk on bond layer on aluminum, embedded in epoxy — is the same, Figure 13. Looking at the bond layer in detail, it shows much blockier crystals with interspersed low-atomic-number regions, as well as small particles, Figure 14. EDS indicates the crystals are essentially Al-O, Figure 15. The piezoceramic shows no visible differences compared to Unirradiated Sample 1, but the bond layer is very different. Indeed, the Si level is very low, and mostly present at the inter-granular regions in the bond layer, so it's possible Si is a minor addition or an artifact of the final polishing step (colloidal silica). The EBSD results, Figure 16, are taken at high magnification around the bonding layer, because of the higher crystallinity of the bonding layer compared to Unirradiated Sample 1. The layer is seen to consist of high-crystal-quality Al_2O_3; the

piezoelectric layer shows more details of the domain structure, thanks to the higher magnification (smaller pixel pitch) in this dataset.

After the observation of Na-K-O needles growing on Unirradiated Sample #1 after several months storage in laboratory air, Unirradiated Sample #5 was re-examined, Figure 17, and is unchanged compared to when freshly polished. Whatever effect led to the growth of features on the as-polished surface in Unirradiated Sample #1 and Irradiated Sample #4, was not present in Unirradiated Sample #5.

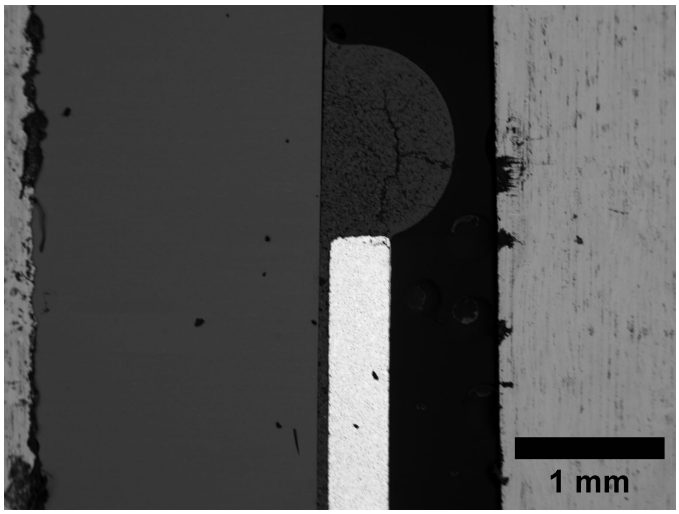

Figure 13. Backscatter electron image of Unirradiated Sample #5, showing details of the bond and piezoceramic.

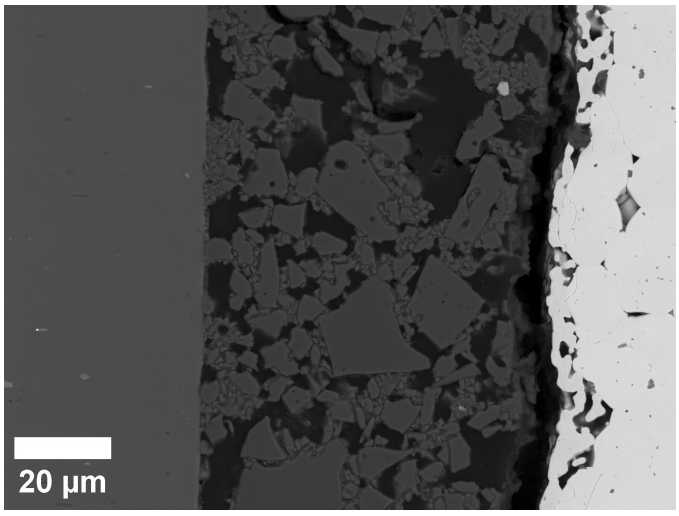

Figure 14. Backscatter electron image of Unirradiated Sample #5. The bond is clearly very crystalline.

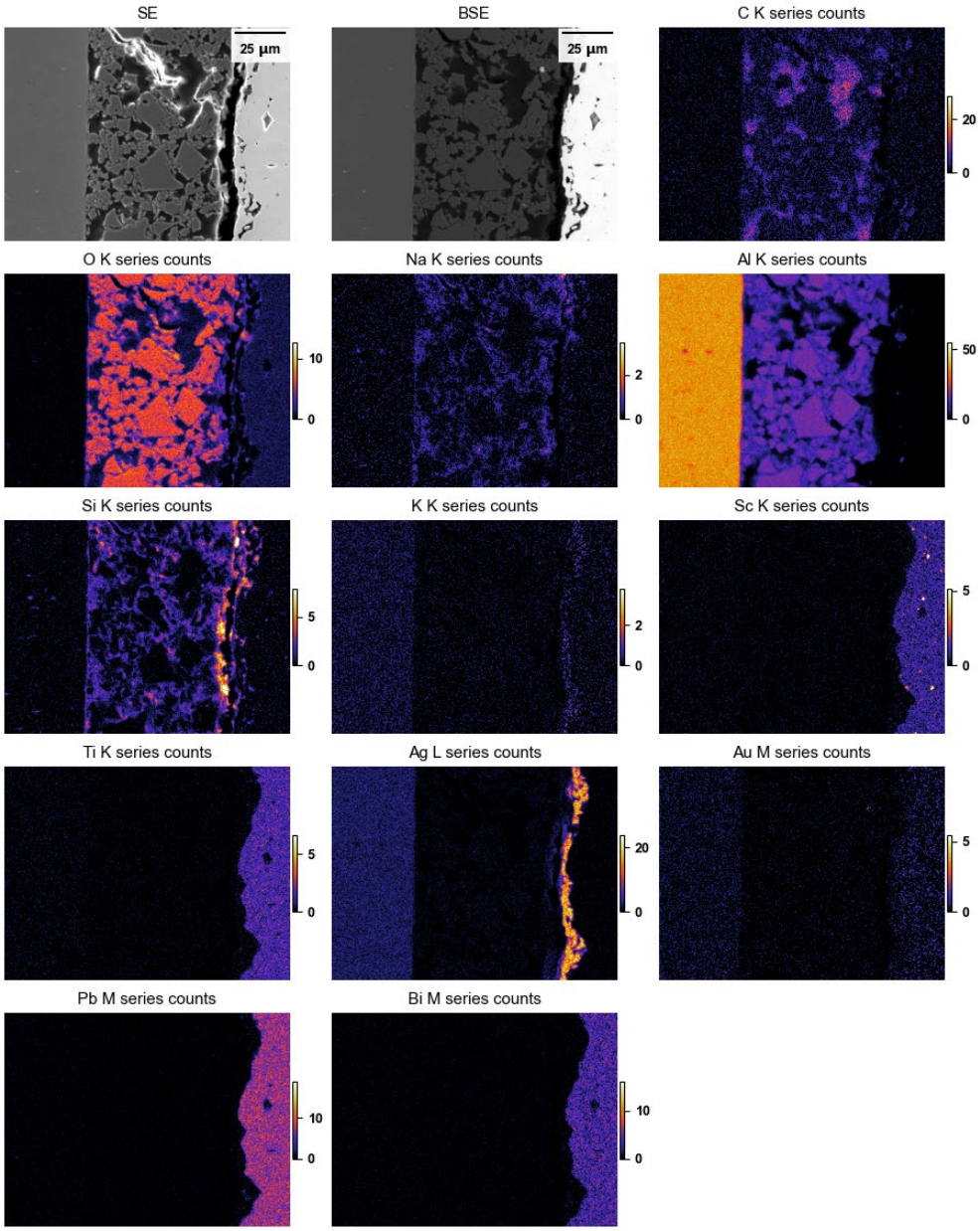

Figure 15. EDS integrated elemental lines extracted from a 15 kV spectrum image from Unirradiated Sample 5.

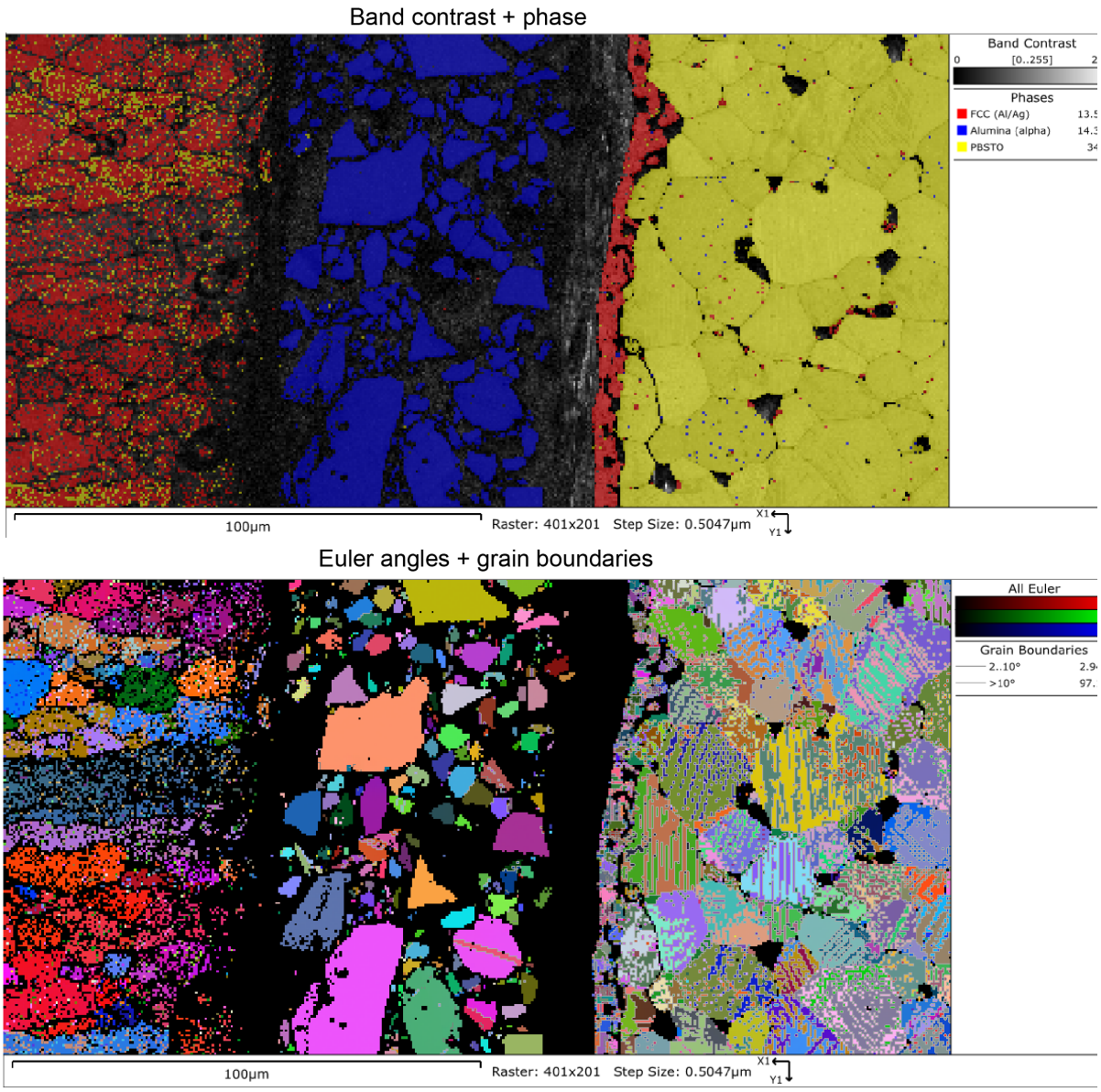

Figure 16. EBSD results from Unirradiated Sample 5. Red phase: FCC, Al or Ag. Blue phase, Al_2O_3. Yellow phase: PBSTO (Pb-Bi-Sc-Ti-O).

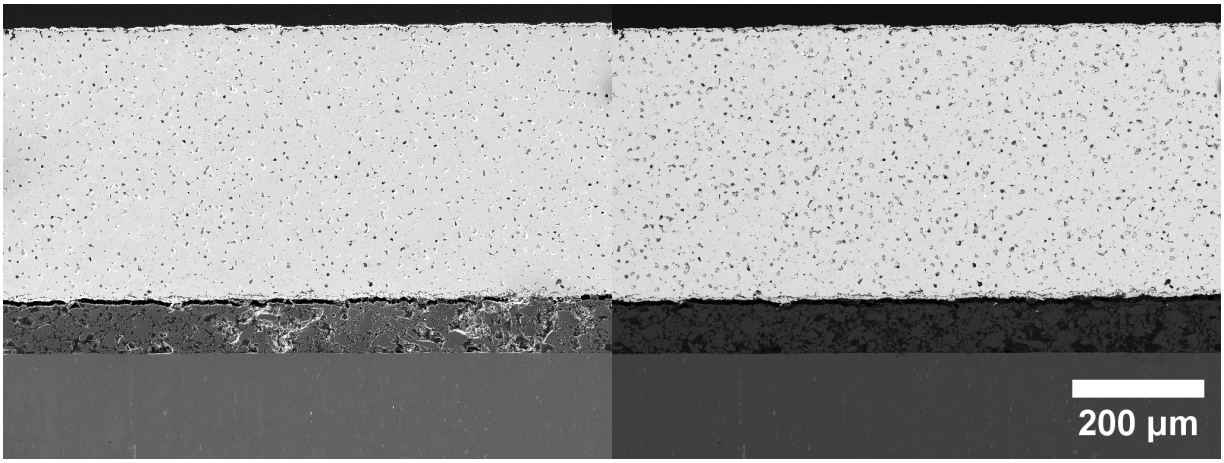

Figure 17. Secondary electron (left) and backscatter electron (right) image of Unirradiated Sample #5 after several months of storage in room air, no changes from imaging when freshly polished.

Unirradiated Sample 11 was also a PBSTO piezoelectric ceramic, and the bonding layer was also Al_2O_3-based. The layers are quite similar, Figure 18. The EDS maps show dense Al-O rich bonding layer and the same PBSTO ceramic, Figure 19 and Figure 20. The EBSD, similarly, shows high quality Al_2O_3 crystals, Figure 21

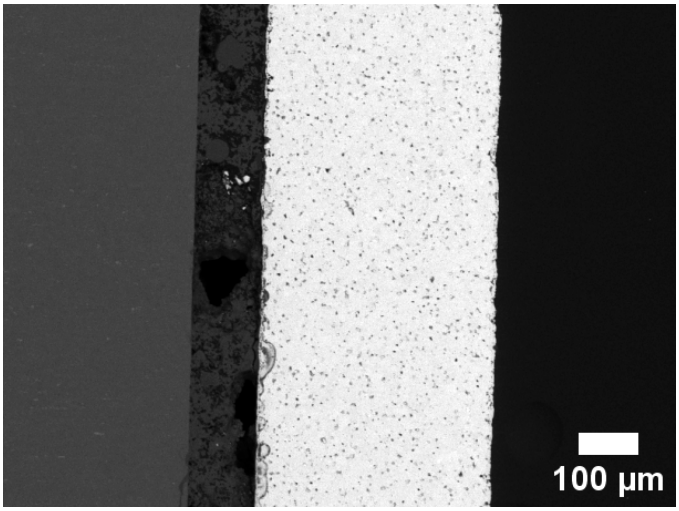

Figure 18. Backscatter electron image of Unirradiated Sample #11, showing details of the bond and piezoceramic.

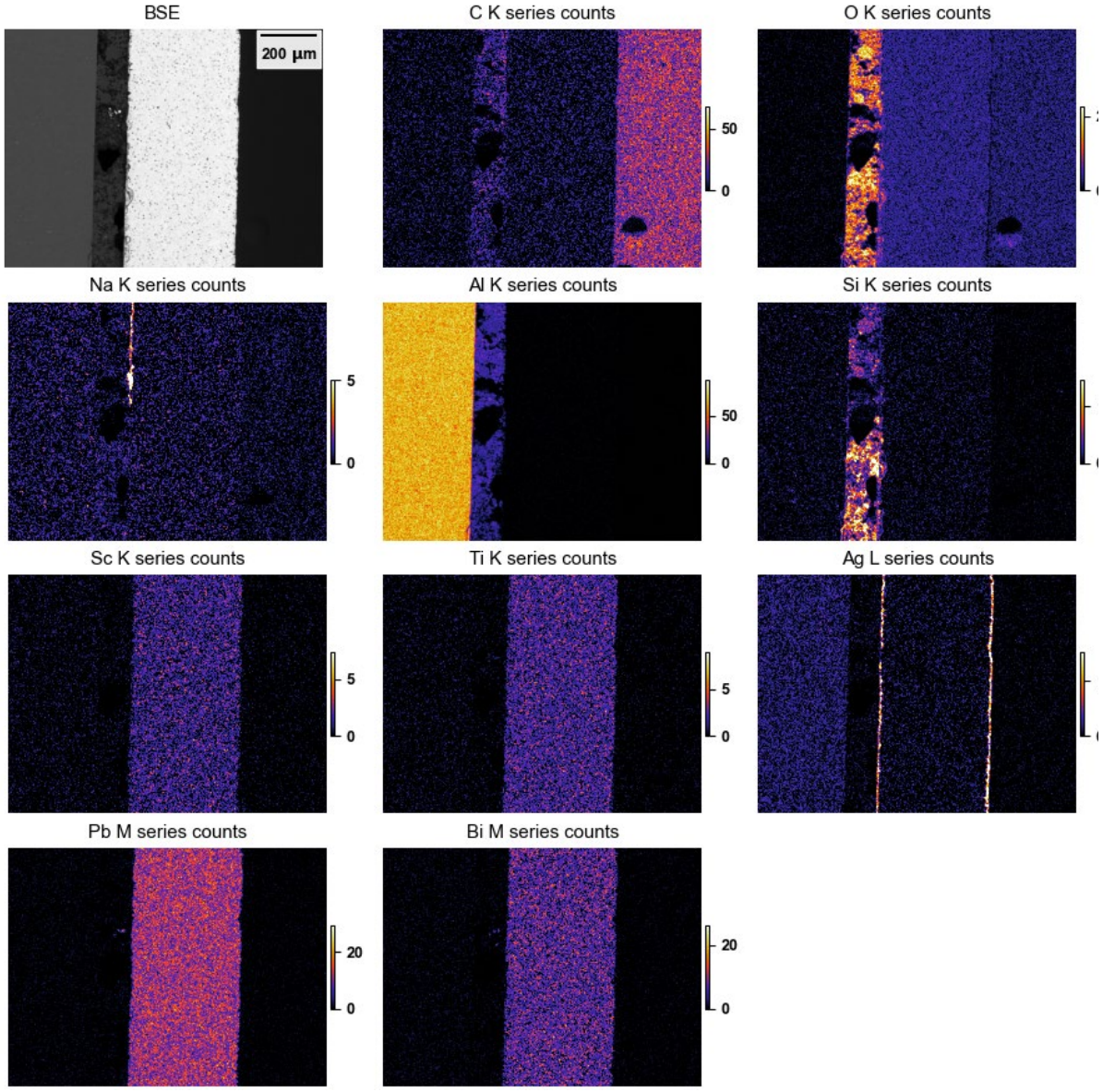

Figure 19. EDS integrated elemental lines extracted from a 10 kV spectrum image from Unirradiated Sample 11.

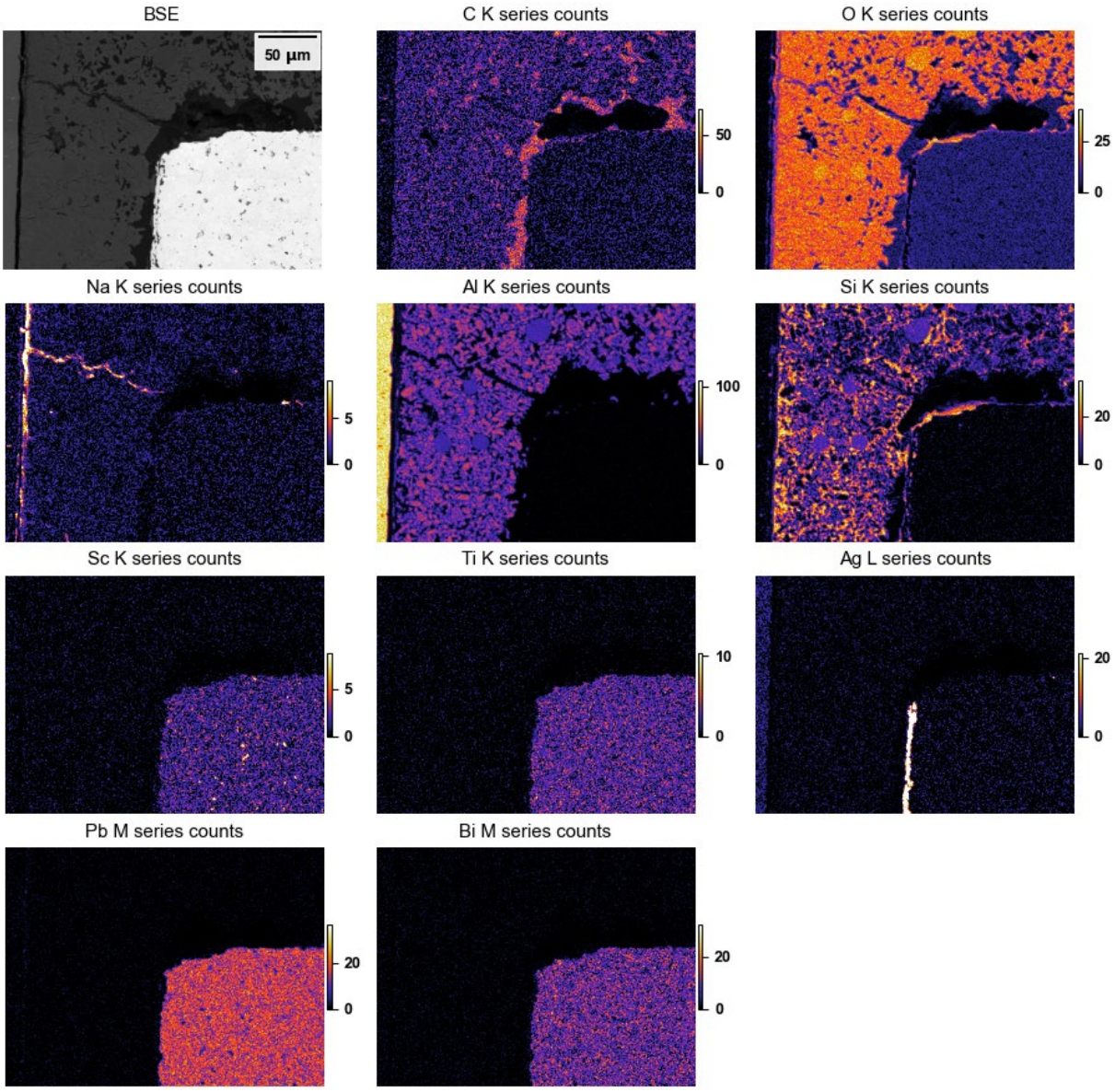

Figure 20. EDS integrated elemental lines extracted from a 10 kV spectrum image from Unirradiated Sample 11.

Band contrast + phase

Euler angles + grain boundaries

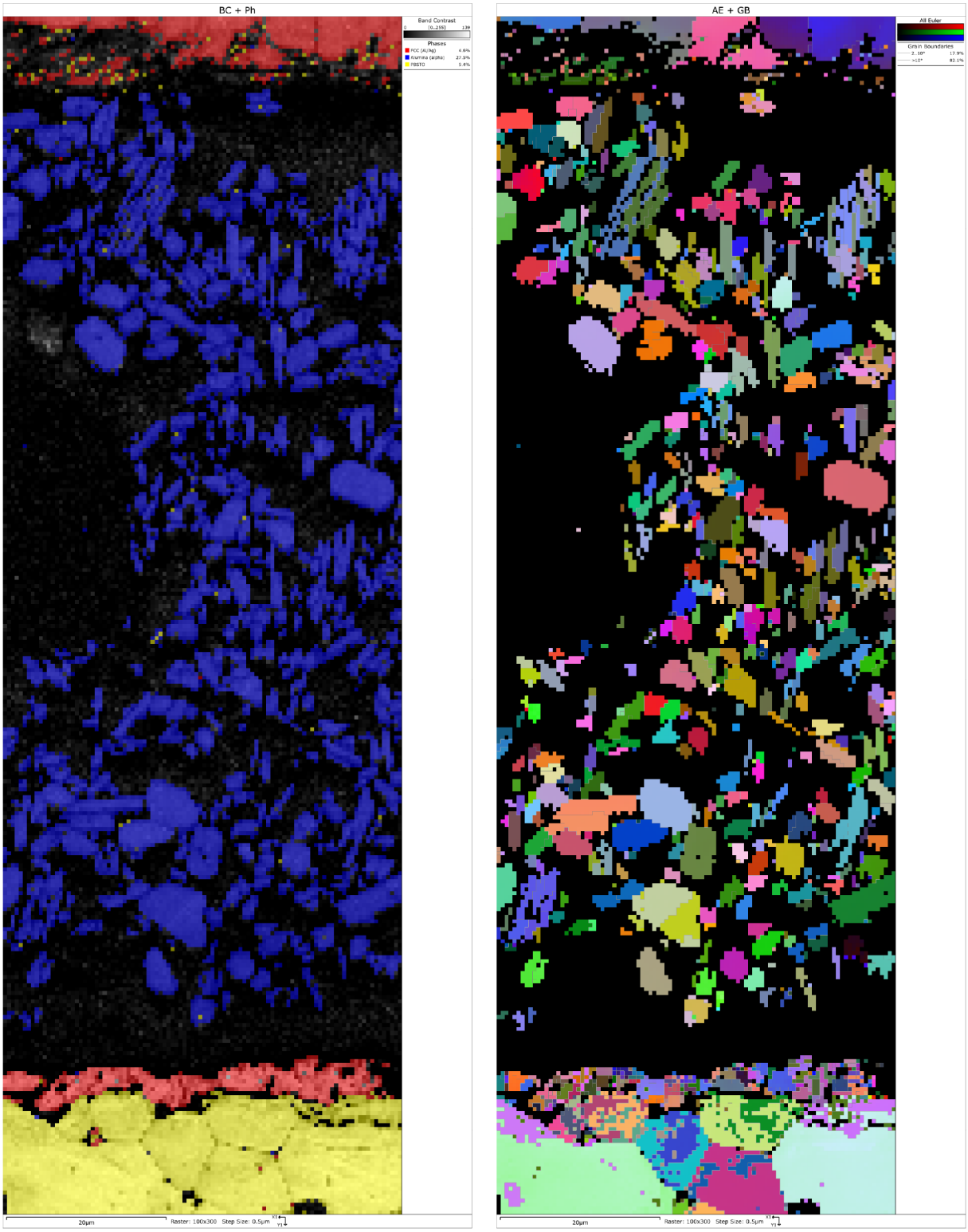

Figure 21. EBSD results from Unirradiated Sample 11. Red phase: FCC, Al or Ag. Blue phase, Al_2O_3. Yellow phase: PBSTO (Pb-Bi-Sc-Ti-O).

Unirradiated Sample 12 shows a zirconia bonding layer; EBSD identified this is tetragonal, but again, electron scattering is less reliable than X-ray scattering and this identification is tentative. The bonding layer is dense and highly crystalline, Figure 22. The BSE image and X-ray maps are in Figure 23 and show the Zr-rich structure. The EBSD, with the unknown phase indexed to tetragonal P 4/mmm zirconia, is in Figure 24.

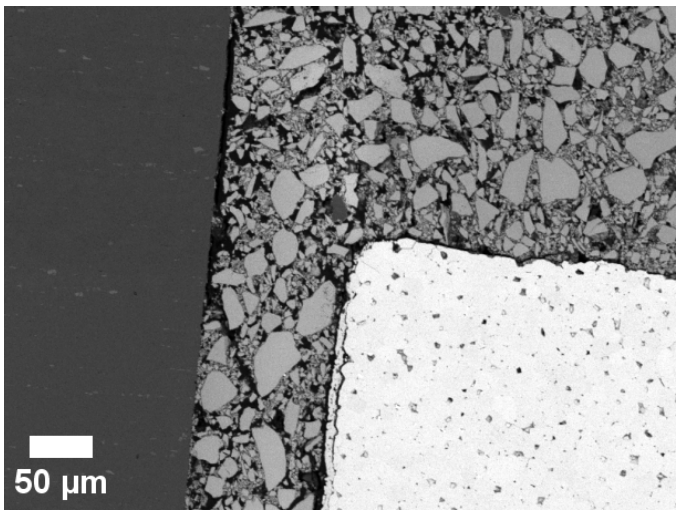

Figure 22. Backscatter electron image of Unirradiated Sample #12, showing details of the bond and piezoceramic.

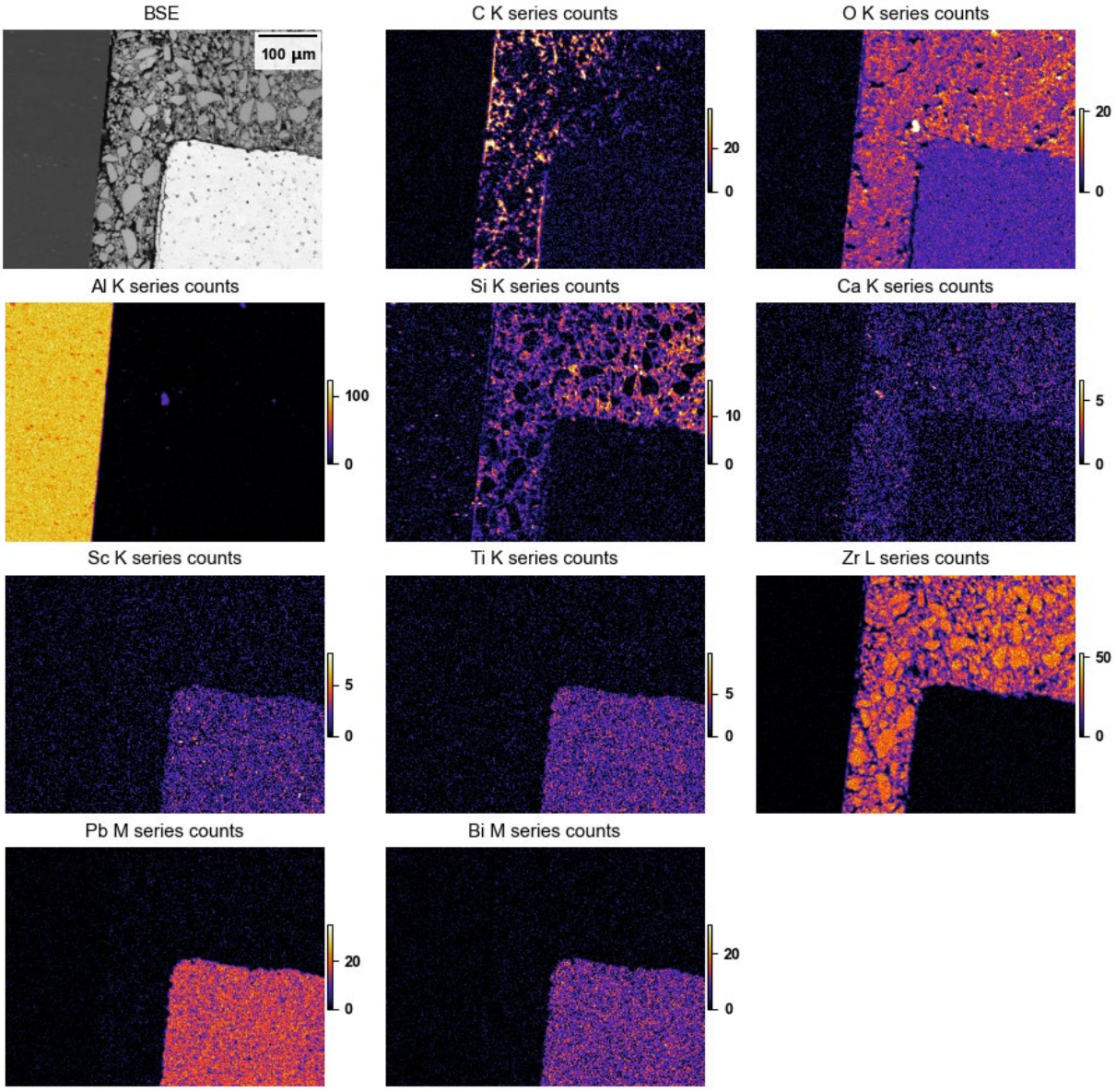

Figure 23. EDS integrated elemental lines extracted from a 10 kV spectrum image from Unirradiated Sample 12.

Band contrast + phase

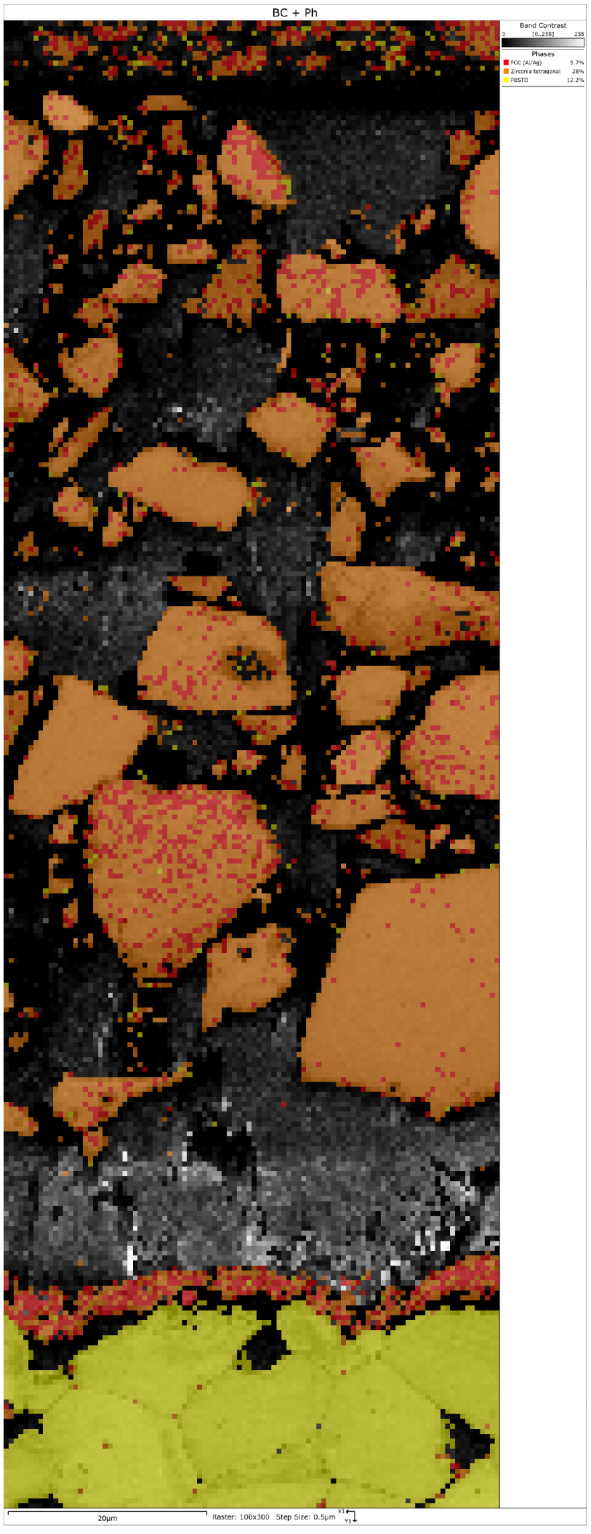

Euler angles + grain boundaries

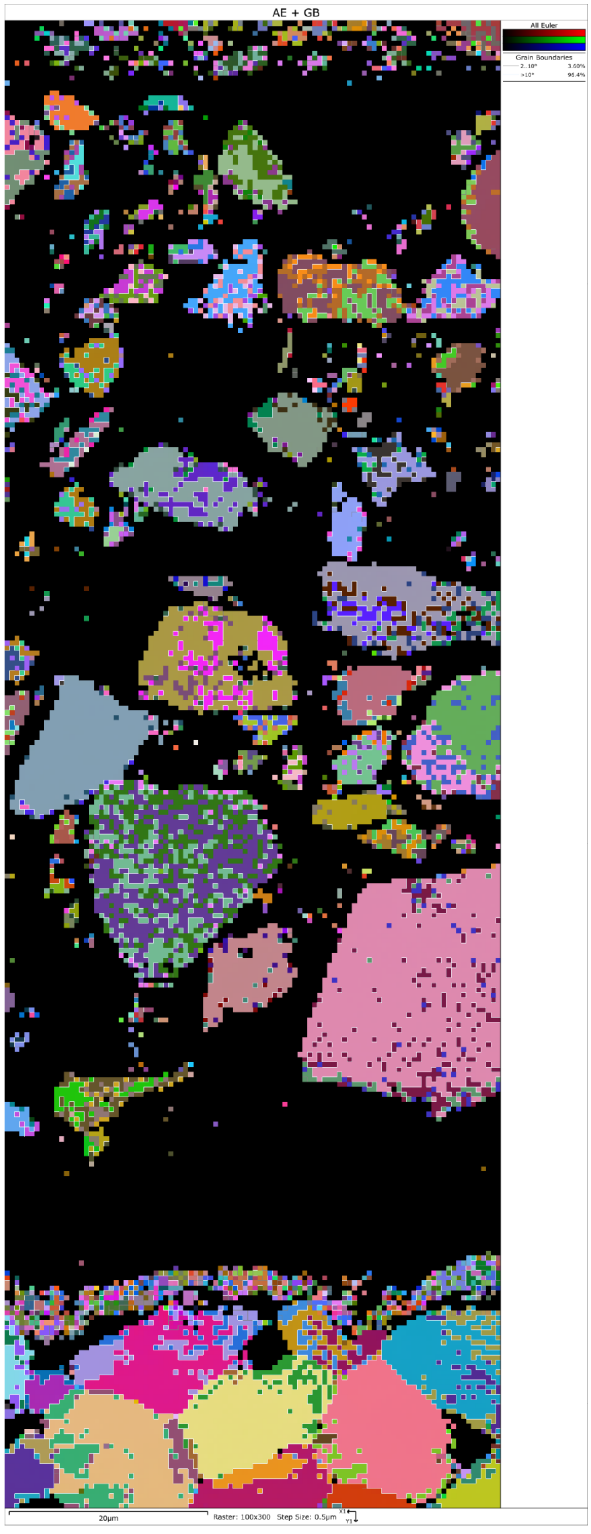

Figure 24. EBSD results from Unirradiated Sample 12. Red phase: FCC, Al or Ag. Orange phase, tetragonal zirconia. Yellow phase: PBSTO (Pb-Bi-Sc-Ti-O).

Unirradiated Sample #13 showed an epoxy bonding layer, and the layer was C-O rich with some S, which is interpreted as a low-temperature-setting S-rich epoxy. The amorphous, featureless epoxy is seen in Figure 25. There is a bright area and some distortion of the image due to the highly insulating epoxy charging up under the beam, despite a thin layer of evaporated carbon. The EDS data, consistent with the other datasets and the epoxy bond, are seen in Figure 26. Because EBSD, by definition, can only analyze crystals, the epoxy was not examined via EBSD.

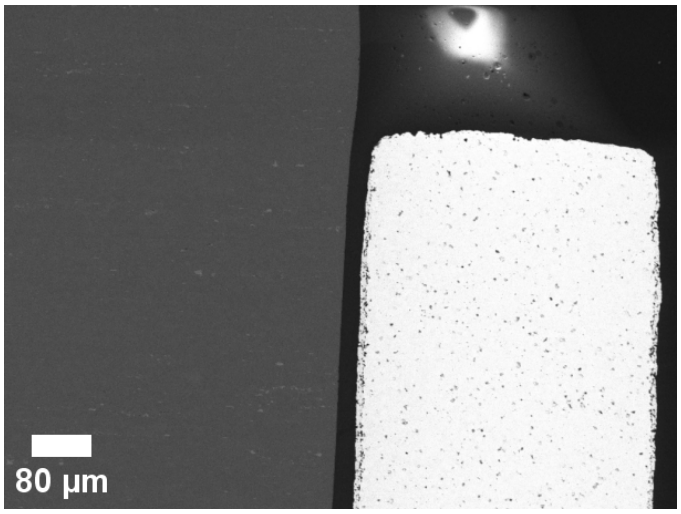

Figure 25. Backscatter electron image of Unirradiated Sample #13, showing details of the bond and piezoceramic. The bright area is charging.

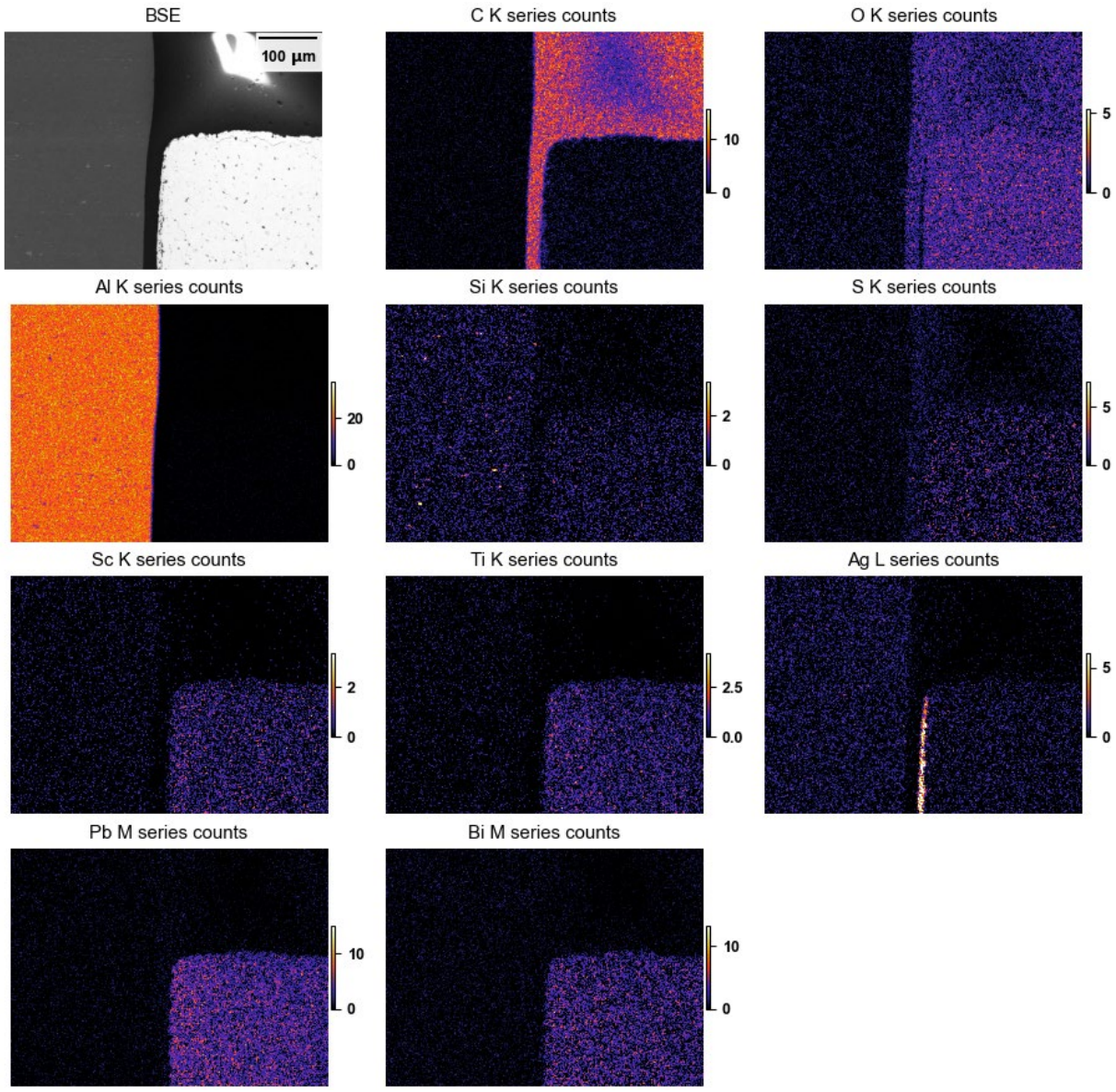

Figure 26. EDS integrated elemental lines extracted from a 10 kV spectrum image from Unirradiated Sample 13.

.

3.2 IRRADIATED

Irradiated Sample #1 showed the PBSTO piezoelectric layer and the Al-Si-Na-K-O bonding layer, Figure 27. The EDS maps indicate a mixed Al-Si-K-Na-O, broadly similar to Unirradiated Sample #1, Figure 28 and Figure 29. Gross differences between Unirradiated Sample #1 and Irradiated Sample #1 are not observed, indicating no gross changes between the specimens. EBSD data will be obtained in the future

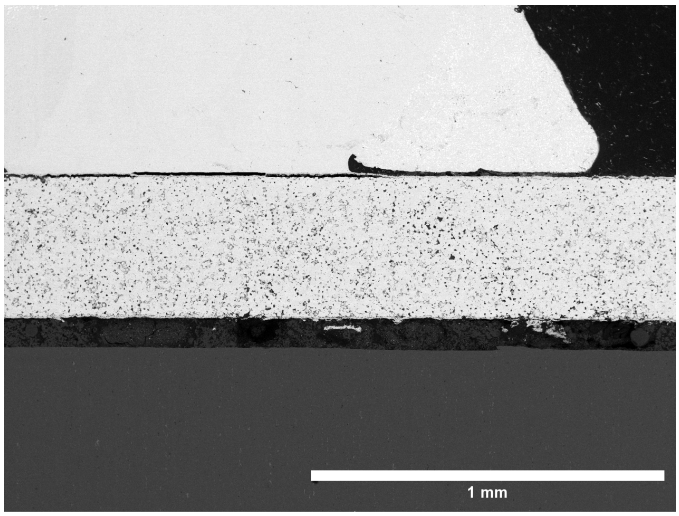

Figure 27. Backscatter electron image of Irradiated Sample #1, showing details of the bond and piezoceramic. The large feature at the top is the solder ball.

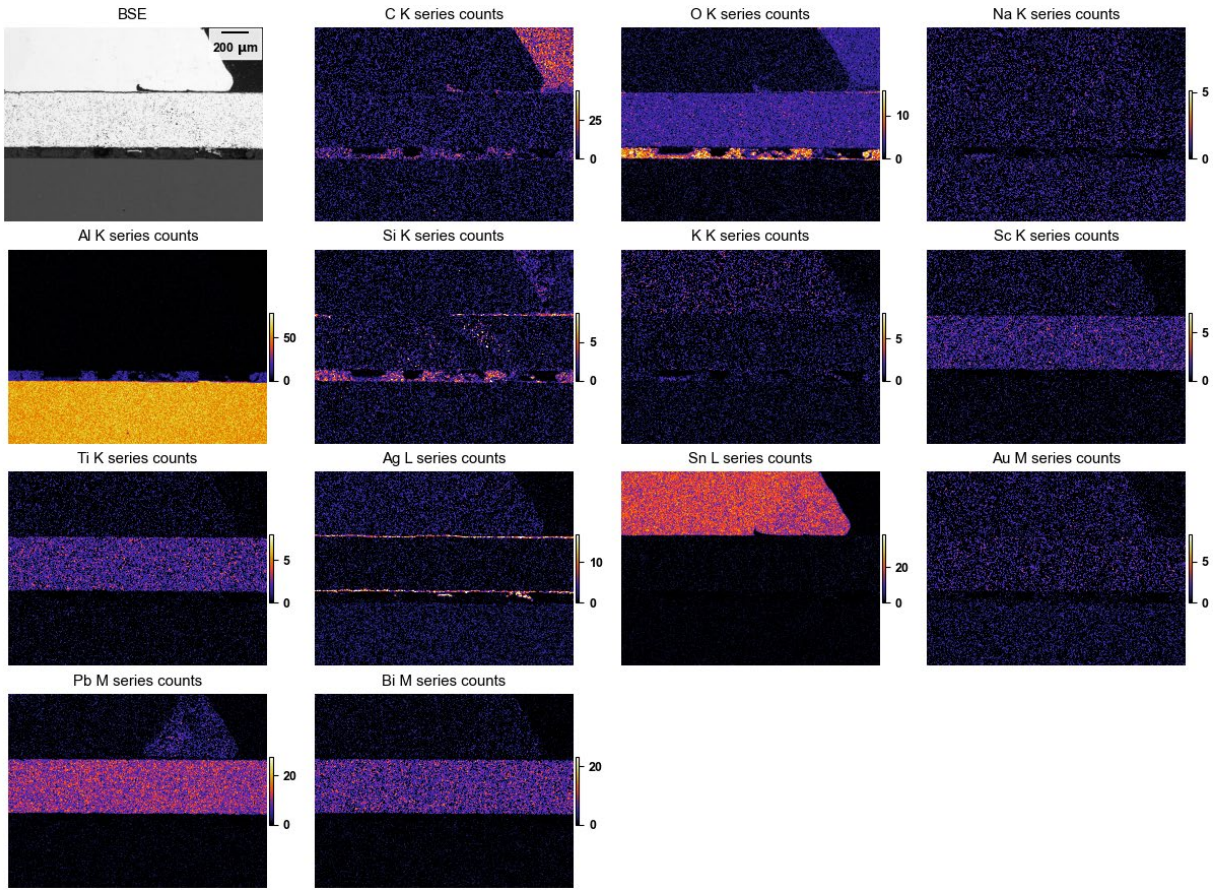

Figure 28. EDS integrated elemental lines extracted from a 10 kV spectrum image from Irradiated Sample 1.

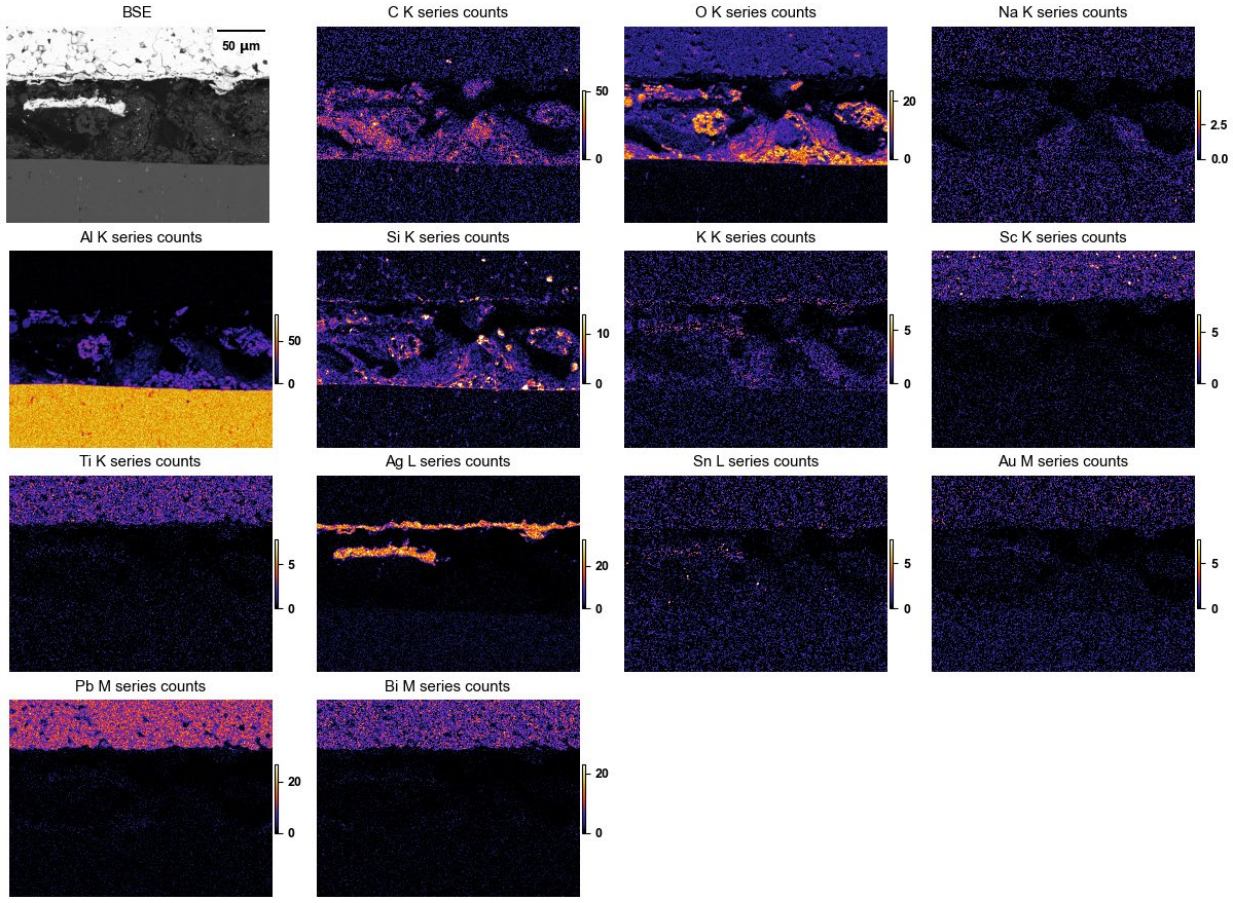

Figure 29. EDS integrated elemental lines extracted from a 10 kV spectrum image from Irradiated Sample 1.

Irradiated Sample #3 showed Nb-O by EDS and is presumed $LiNbO_3$; Li is essentially undetectable with standard SDD detectors. This sample arrived at ORNL LAMDA from NCSU PULSTAR broken off its substrate, so analysis of the bonding is not possible. The ceramic itself also showed cracks. The electrodes appear to be AuCr rather than Ag. This indicates significant brittleness in the layer.

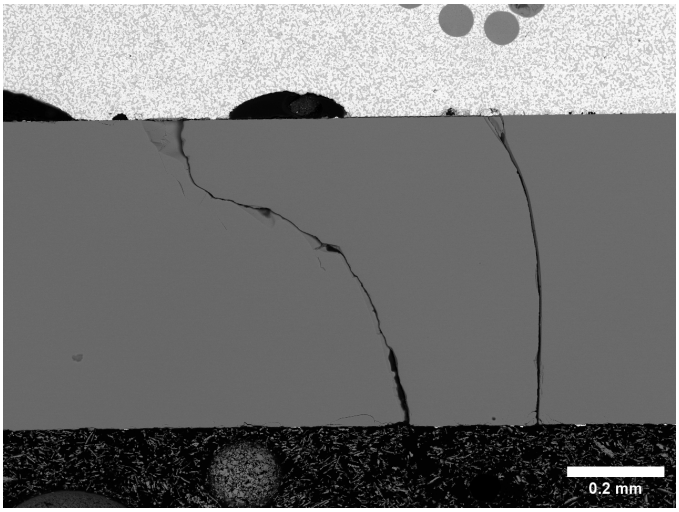

Figure 30. Backscatter electron image of Irradiated Sample #3, showing that the piezoceramic broke off the bond during transport. The black region at the bottom is conductive epoxy. The bright region at the top is the solder ball.

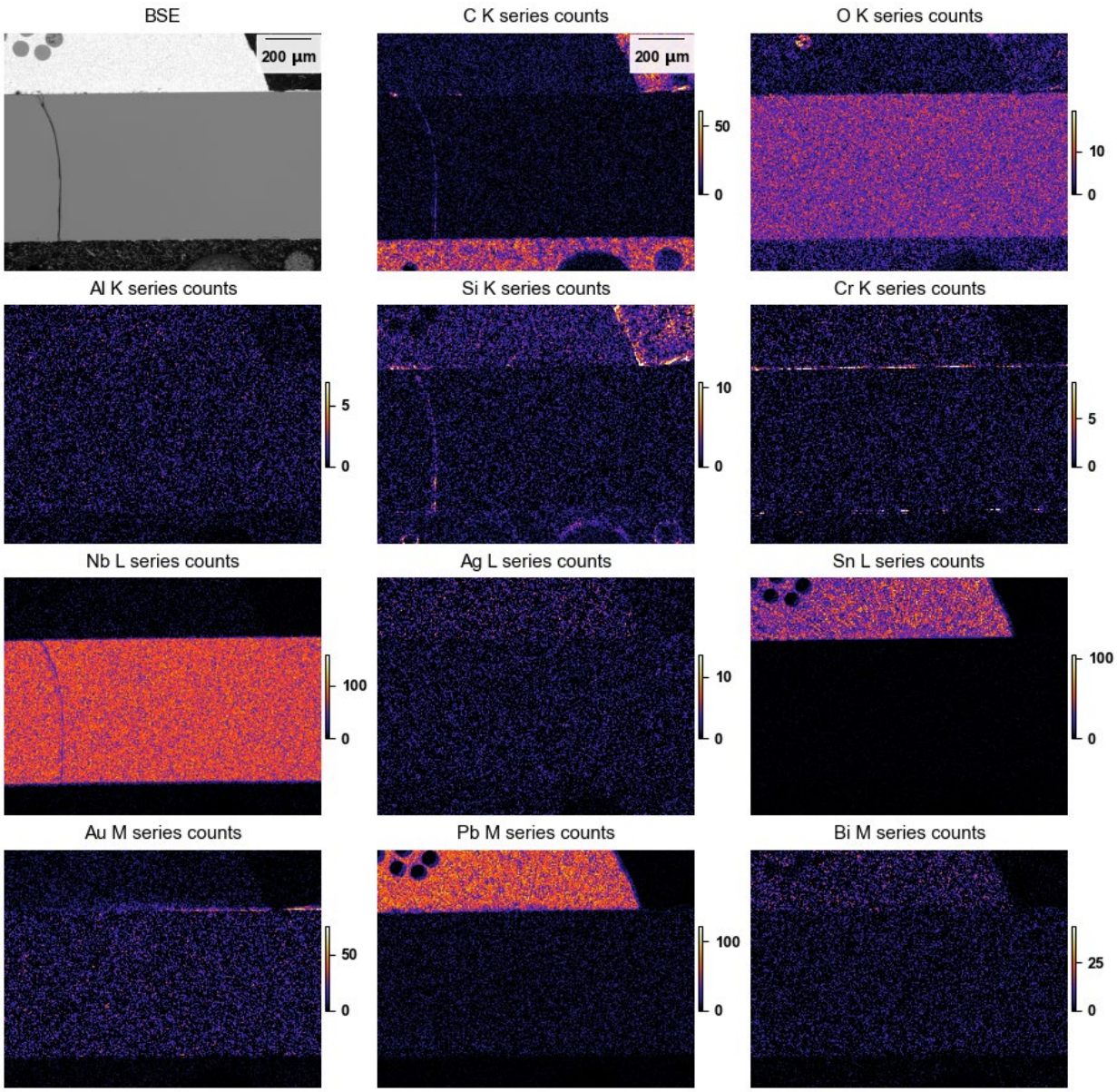

Figure 31. EDS integrated elemental lines extracted from a 20 kV spectrum image from Irradiated Sample #3.

Irradiated Sample #4 was PBSTO with a highly crystalline and dense Al-O primary bonding layer that contained some Na and Si; this is grossly similar to Unirradiated Sample #5, Figure 32. However, this sample grew complex Na-O "flowers" at the piezoelectric/bonding layer interface, Figure 33. EDS, Figure 34, shows the bonding layer is similar to Unirradiated Sample #5, except for the Na-O rich flowers sprouting from the bond / piezoceramic interface.

On the one hand, these seems similar to Unirradaited Sample #1, where Na-K-O needles grew across the piezoceramic surface, but is distinct in that the growths are limited to the bond/piezoceramic interface, and do not seem to contain K.

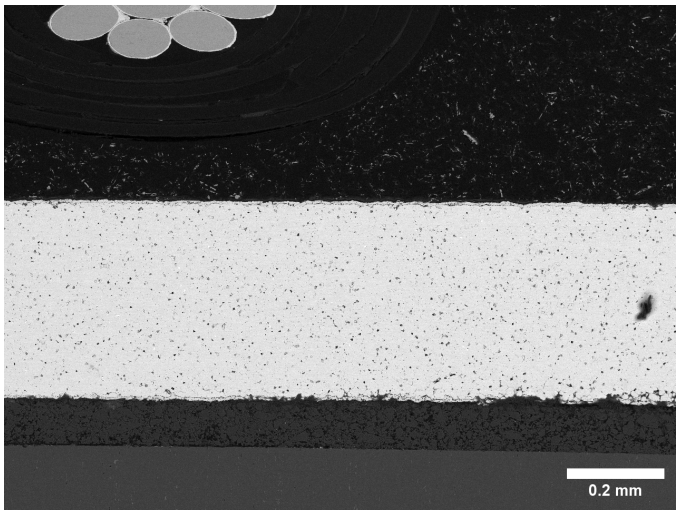

Figure 32. Backscatter electron image of Irradiated Sample #4, showing details of the bond and piezoceramic. The large feature at the top is a contact wire attached to the solder ball and cutting the plane of polish.

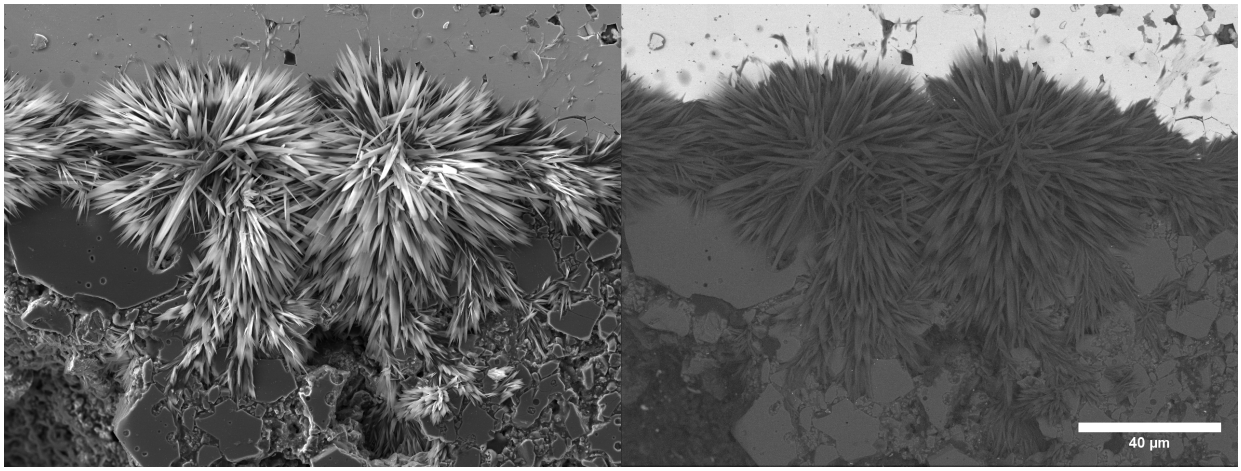

Figure 33. Secondary electron (left) and backscatter electron (right) image of Irradiated Sample #4, showing the Na-O "flowers" growing at the bond / piezoceramic interface.

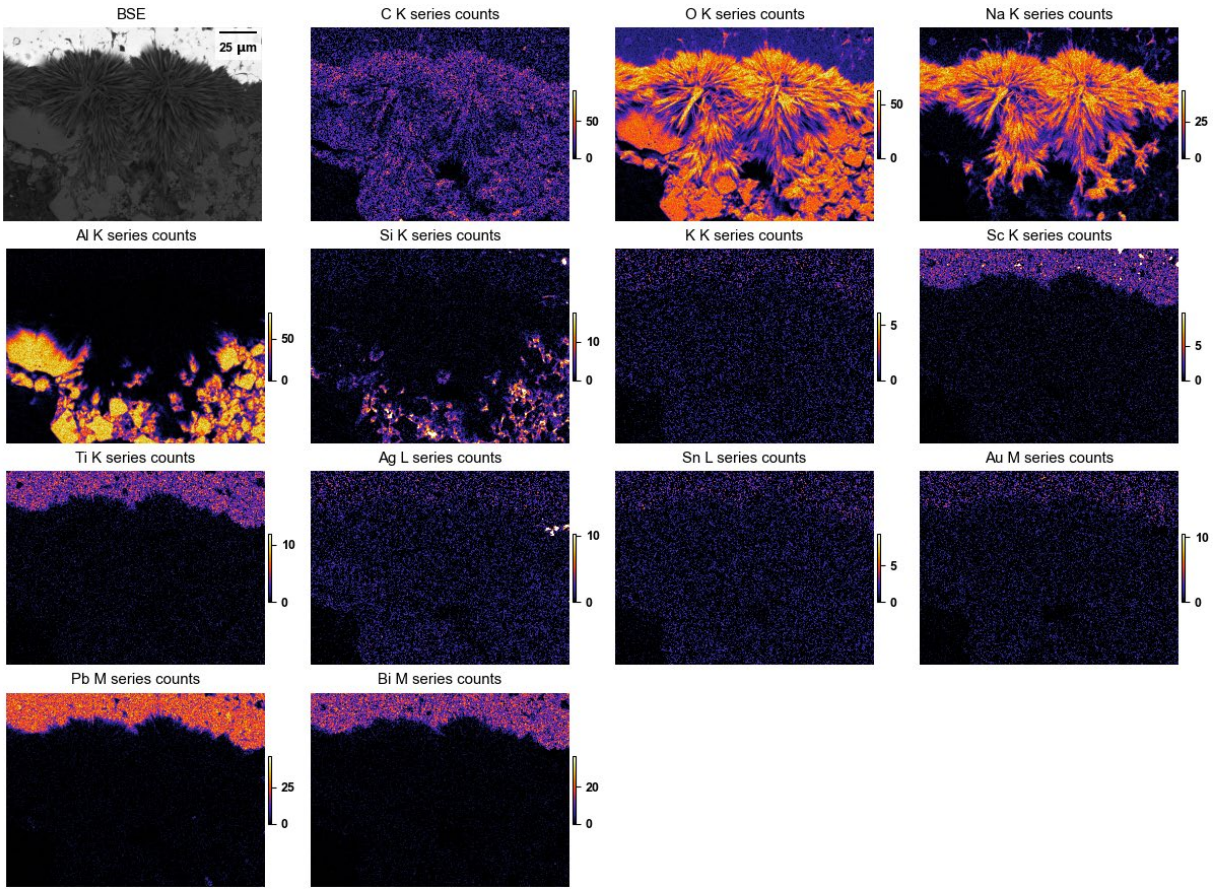

Figure 34. EDS integrated elemental lines extracted from a 10 kV spectrum image from Irradiated Sample #4, showing the Na-O rich growths. Detector is an 12 o'clock high orientation, resulting in shadowing towards the bottom of the image.

Irradiated Sample #5 is PBSTO on a zirconia bond layer, Figure 35. X-ray mapping confirms a Zr-O bonding layer with small amounts of Ca and Si, Figure 36; this is essentially identical to Unirradiated Sample #12. The EBSD of this sample, Figure 37, shows a large amount of misindexing between the Al and ZrO_2 phases; this is because of low pattern quality in the aluminum, perhaps due to irradiation, and due to some pseudosymmetries between the cubic Al and tetragonal ZrO_2 reflectors. Comparison of monoclinic and orthorhombic ZrO_2 solutions vs. tetragonal (P 4/mmm) ZrO_2 solutions on a few individual patterns indicate tetragonal is a better match. Overall, EBSD confirms the layer contains blocky, high-quality tetragonal ZrO_2 particles.

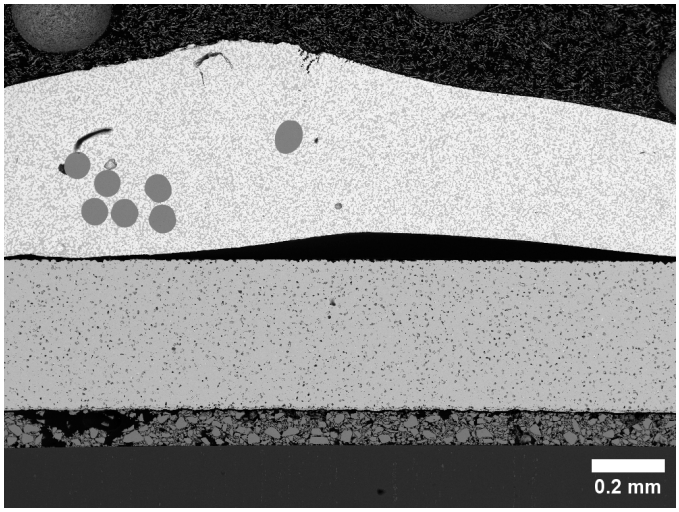

Figure 35. Backscatter electron image of Irradiated Sample #5, showing details of the bond and piezoceramic. The large feature at the top is the solder ball.

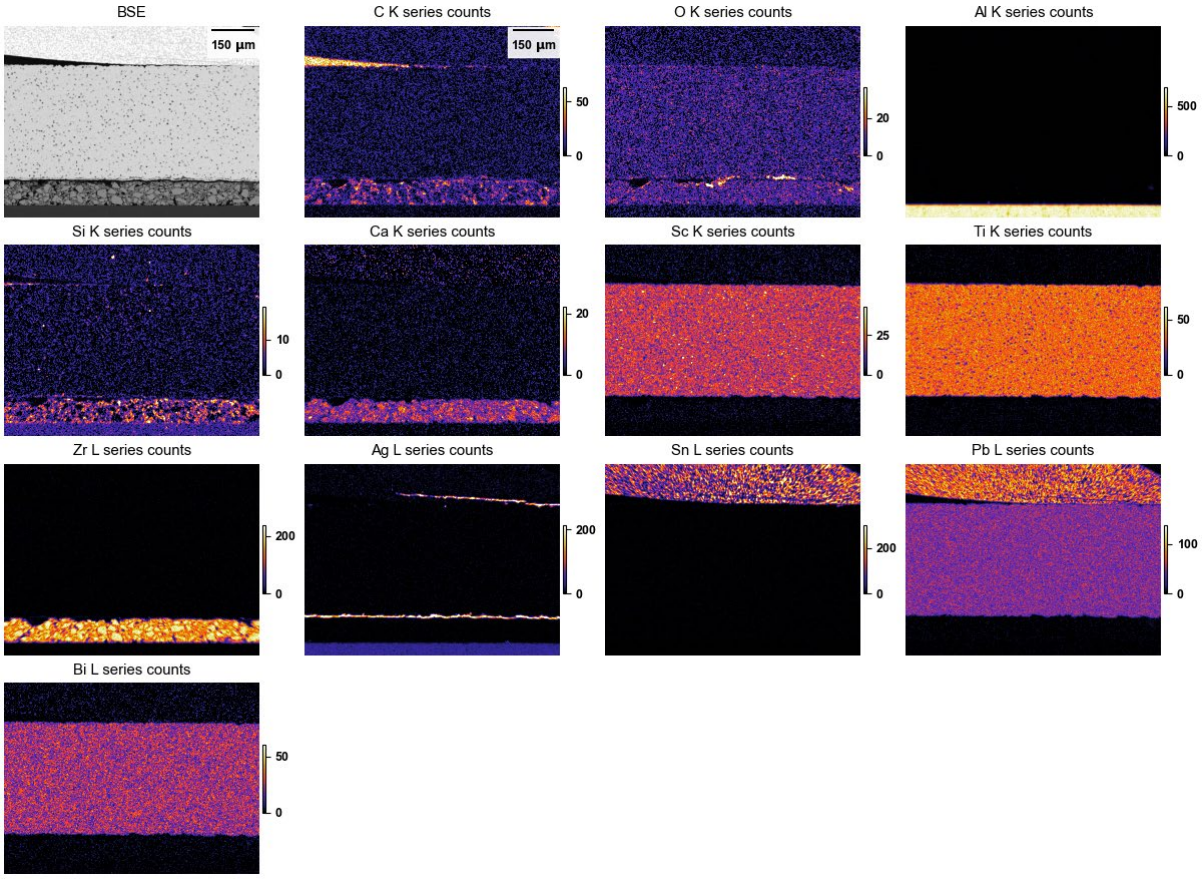

Figure 36. EDS integrated elemental lines extracted from a 30 kV spectrum image from Irradiated Sample #5, showing a solder ball, PBSTO layer, and Zr(-Ca-Si)-O bond.

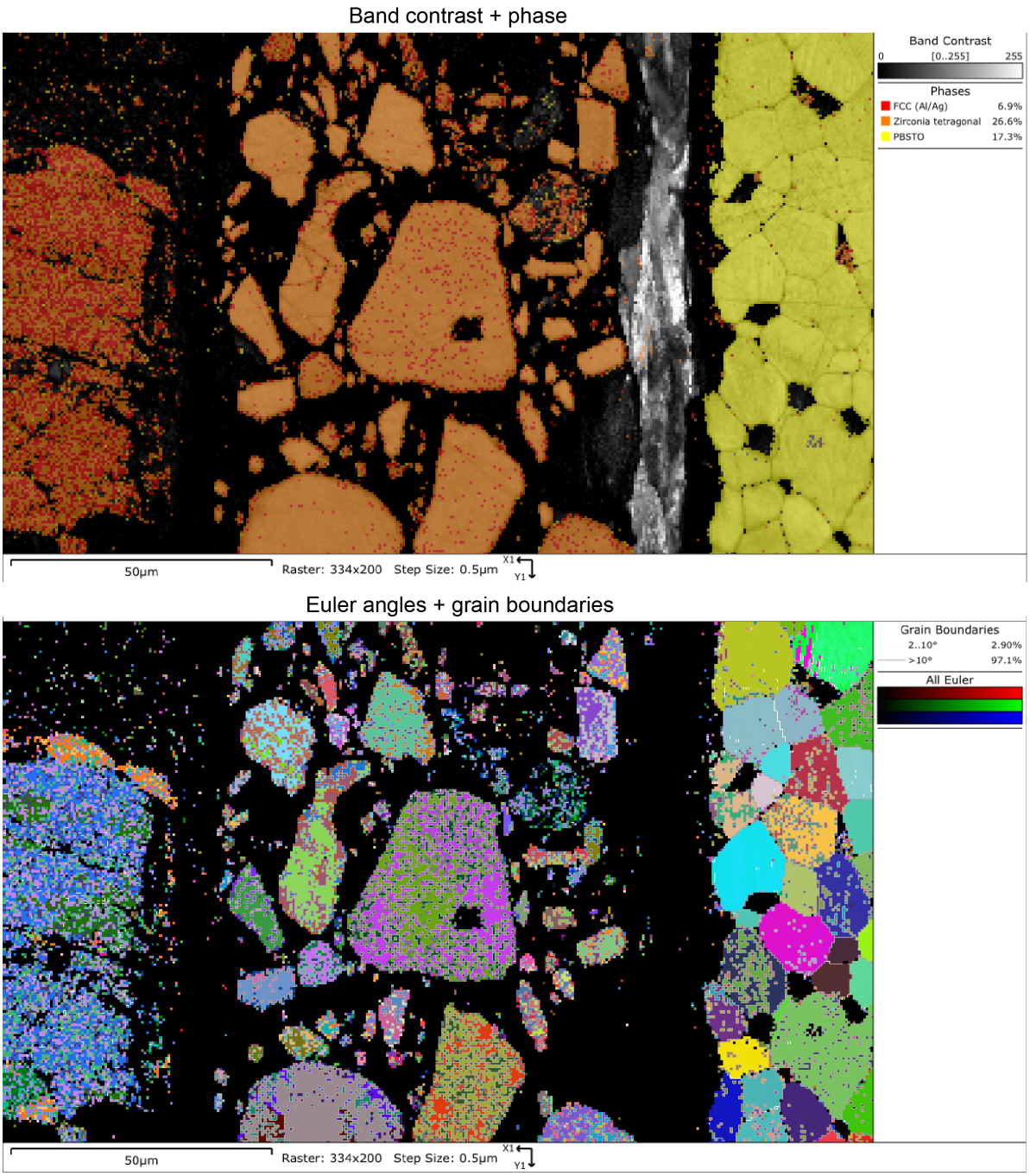

Figure 37. EBSD results from Irradiated Sample #5 Red phase: FCC, Al or Ag. Orange phase, tetragonal zirconia. Yellow phase: PBSTO (Pb-Bi-Sc-Ti-O). Significant orange/red speckle (misindexing) is due to pseudosymmetric reflector positions between <101> Al and <100> ZrO_2 and due to poor pattern quality in the irradiated Al.

Irradiated Sample #6 is PBSTO, with an epoxy bonding layer, Figure 38. X-ray analysis found the bonding layer was C-O(-S) rich, consistent again with epoxy, Figure 39.

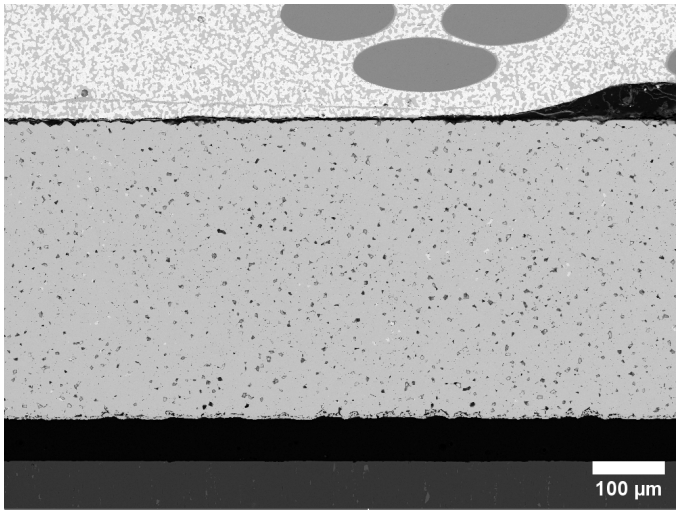

Figure 38. Backscatter electron image of Irradiated Sample #5, showing details of the bond and piezoceramic. The feature at the top is the solder ball.

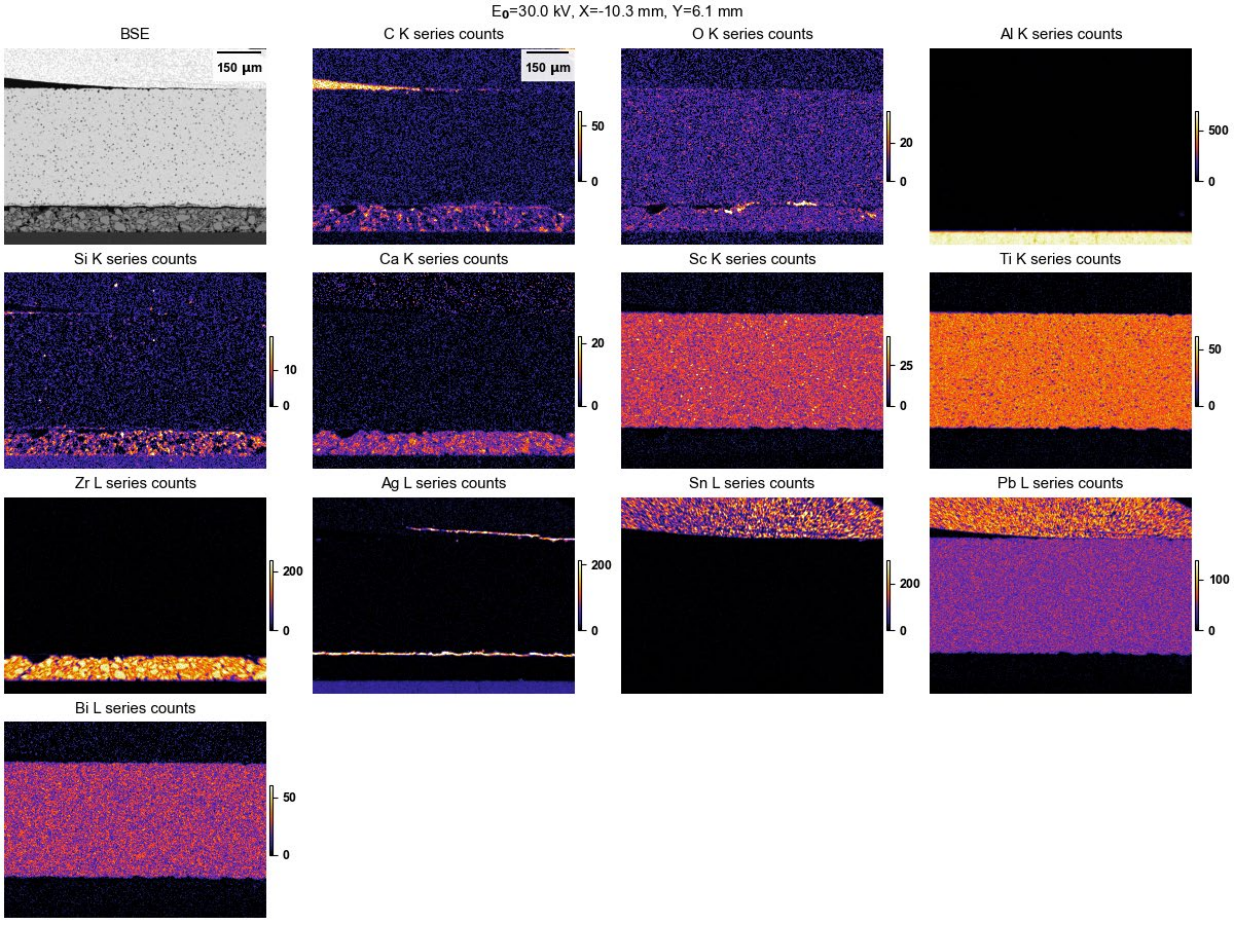

Figure 39. EDS integrated elemental lines extracted from a 20 kV spectrum image from Irradiated Sample #5, showing a solder ball, PBSTO layer, and Zr(-Ca-Si)-O bond.

Irradiated Sample #7 is another Nb-O ceramic, presumably $LiNbO_3$, and has an epoxy bonding layer. The electrodes appear to be AuCr rather than Ag. The epoxy is featureless, but appears to have maintained a good bond. The piezoceramic is not cracked, unlike Irradiated Sample #3 above.

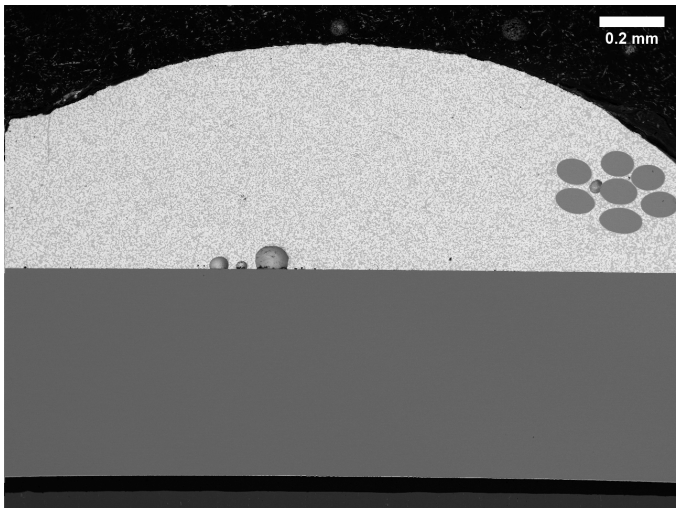

Figure 40. Backscatter electron image of Irradiated Sample #7, showing details of the bond and piezoceramic. The solder ball is at the top.

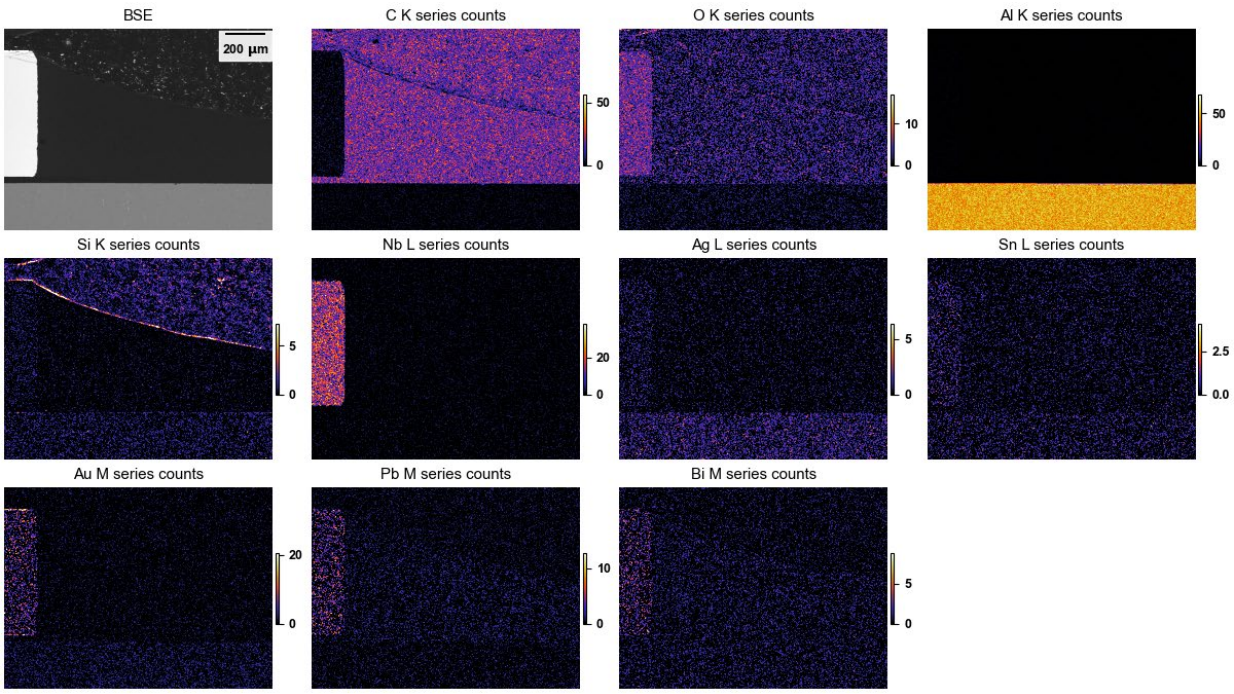

Figure 41. EDS integrated elemental lines extracted from a 10 kV spectrum image from Irradiated Sample #7.

Irradiated Sample #8 is very similar to Irradiated Sample #7, Figure 42. It is again $LiNbO_3$ with AuCr electrodes and an epoxy bonding layer; Figure 43. The bond stayed attached and the ceramic does not appear cracked. The main difference between Irradiated Sample #7 and Irradiated Sample #8 appears to be that #7 has a Pb-Sn solder ball, and #8 has a Sn-Cu solder ball.

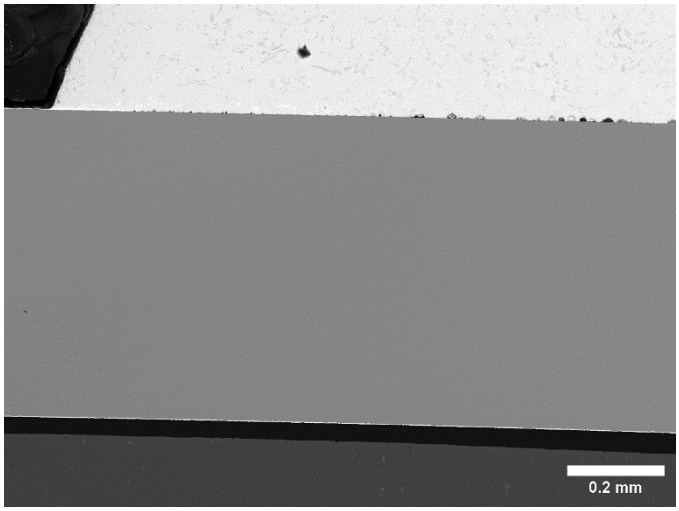

Figure 42. Backscatter electron image of Irradiated Sample #8, showing details of the bond and piezoceramic. The solder ball is at the top.

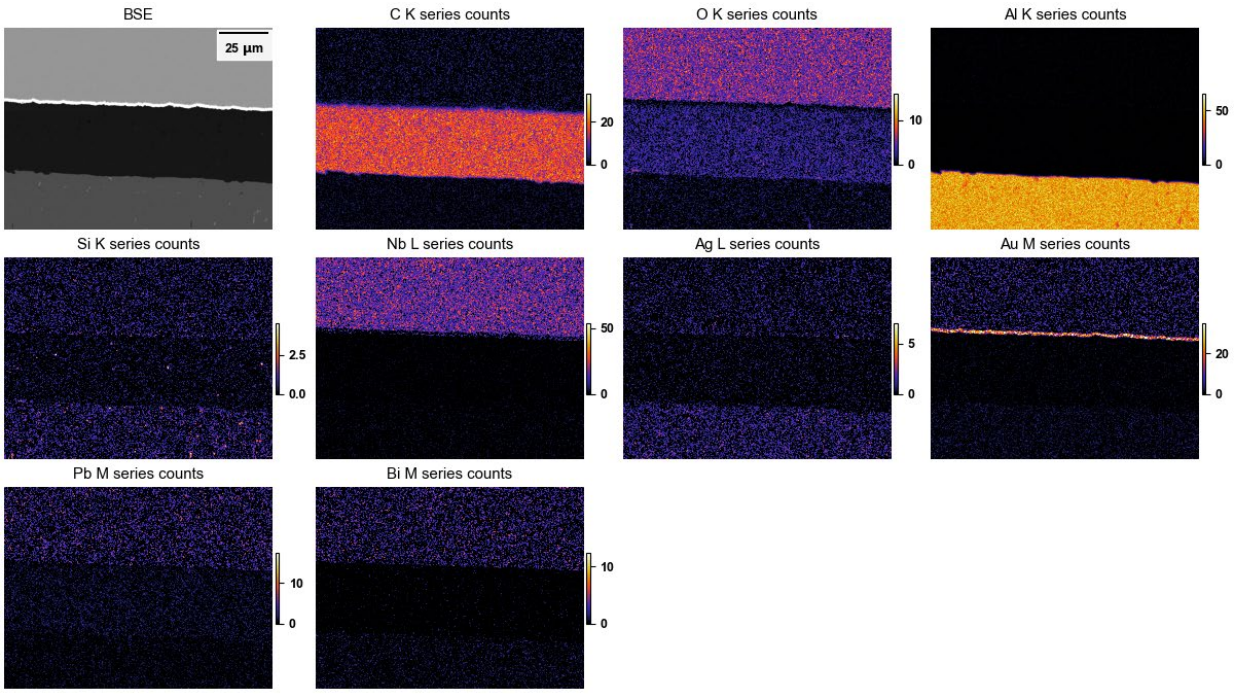

Figure 43. EDS integrated elemental lines extracted from a 10 kV spectrum image from Irradiated Sample #8.

4. SUMMARY AND ONGOING WORK

The samples appear to be from two different types: $LiNbO_3$ or $(Pb,Bi)(Ti,Sc)O_3$, PBSTO. $LiNbO_3$ samples were only examined in the irradiated state, but the PBSTO layers showed no gross differences in the irradiated and unirradiated state. EBSD mapping and BSE imaging of the domain structures, and S/TEM analysis, is planned to examine difference in the domain structures, grain boundaries, and the evolution of irradiation-induced defects in the PBSTO and $LiNbO_3$ samples.

The bonding layers consisted of Al-Si-K-Na-O, Al-O, Zr-O, or epoxy. For the Al-O, Zr-O, and epoxy layers, no obvious differences were seen before and after irradiated. However, the Na-bearing layer showed growth of Na-O "flowers" at the bond/piezoceramic interface after polishing in the irradiated state, and Na-K-O needles across the piezoceramic after several months' storage in the unirradiated state. The mechanisms for these feature growths are likely related to humidity in storage. Further, the mechanisms causing the differences between the Na-K-O needles on Unirradiated Sample #1 and Na-O flowers on Irradiated Sample #4 are as yet unclear.